

AD-A150 793

SURFACE PRESSURE PRODUCED BY SPACE TRANSPORTATION
SYSTEM FLIGHT 41B(U) WESTON OBSERVATORY MA
F A CROWLEY ET AL. 01 AUG 84 SCIENTIFIC-1

1/1

UNCLASSIFIED

AFGL-TR-84-0213 F19628-84-C-0011

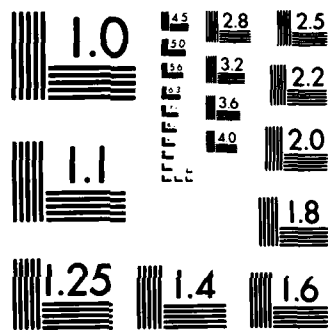
F/G 22/4

NL

END

FORM 1

1/1



MICROCOPY RESOLUTION TEST CHART
NATIONAL BUREAU OF STANDARDS 1963 A

2

AFGL-TR-84-0213

SURFACE PRESSURE PRODUCED BY SPACE TRANSPORTATION SYSTEM FLIGHT 41B

Francis A. Crowley
Eugene B. Hartnett
Michael A. Fisher

Weston Observatory
Department of Geology and Geophysics
Boston College
381 Concord Road
Weston, Massachusetts 02193

1 August 1984

Scientific Report No. 1

Approved for Public Release; Distribution Unlimited

Air Force Geophysics Laboratory
Air Force Systems Command
United States Air Force
Hanscom AFB, Massachusetts 01731

DTIC
ELECTE
MAR 01 1985
S
E
D

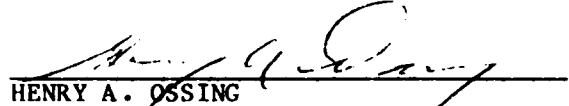
AD-A150 793

DTIC FILE COPY

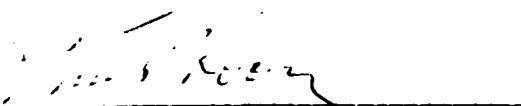
CONTRACTOR REPORTS

This technical report has been reviewed and is approved for publication.


HENRY A. OSSING
Contract Manager


HENRY A. OSSING
Chief, Solid Earth Geophysics Branch

FOR THE COMMANDER


THOMAS P. ROONEY
Acting Director
Earth Sciences Division

This report has been reviewed by the ESD Public Affairs Office (PA) and is releasable to the National Technical Information Service (NTIS).

Qualified requestors may obtain additional copies from the Defense Technical Information Center. All other should apply to the National Technical Information Service.

If your address has changed, or if you wish to be removed from the mailing list, or if the addressee is no longer employed by your organization, please notify AFGL/DAA, Hanscom AFB, MA 01731. This will assist us in maintaining a current mailing list.

UNCLASSIFIED

SECURITY CLASSIFICATION OF THIS PAGE

REPORT DOCUMENTATION PAGE

1a. REPORT SECURITY CLASSIFICATION UNCLASSIFIED		1b. RESTRICTIVE MARKINGS	
2a. SECURITY CLASSIFICATION AUTHORITY		3. DISTRIBUTION/AVAILABILITY OF REPORT APPROVED FOR PUBLIC RELEASE ; DISTRIBUTION UNLIMITED	
2b. DECLASSIFICATION/DOWNGRADING SCHEDULE			
4. PERFORMING ORGANIZATION REPORT NUMBER(S)		5. MONITORING ORGANIZATION REPORT NUMBER(S) AFGL-TR-84-0213	
6a. NAME OF PERFORMING ORGANIZATION Weston Observatory Boston College	6b. OFFICE SYMBOL <i>(If applicable)</i>	7a. NAME OF MONITORING ORGANIZATION Air Force Geophysics Laboratory Terrestrial Sciences Division (LWH)	
6c. ADDRESS (City, State and ZIP Code) 381 Concord Road Weston, MA 02193		7b. ADDRESS (City, State and ZIP Code) Hanscom AFB, MA 01731 Monitor: Henry A. Ossing	
8a. NAME OF FUNDING/SPONSORING ORGANIZATION Same as Block 7a	8b. OFFICE SYMBOL <i>(If applicable)</i>	9. PROCUREMENT INSTRUMENT IDENTIFICATION NUMBER F19628-84-C-0011	
8c. ADDRESS (City, State and ZIP Code)		10. SOURCE OF FUNDING NOS	
		PROGRAM ELEMENT NO	PROJECT NO
		62101F	7600
		TASK NO	WORK UNIT NO
		09	AF
11. TITLE (Include Security Classification) Produced by *STS Flight 41-B (U) Surface Pressure			
12. PERSONAL AUTHOR(S) CROWLEY, Francis A. ; HARTNETT, Eugene B. : ** FISHER, Michael A., Capt, USAF			
13a. TYPE OF REPORT Scientific Report No 1	13b. TIME COVERED FROM Nov 83 to Mar 84	14. DATE OF REPORT (Yr, Mo, Day) 84/08/01	15. PAGE COUNT 72
16. SUPPLEMENTARY NOTATION *Block 11 STS (Space Transportation System) ** Block 12, Headquarters, Space Division			
17. COSATI CODES		18. SUBJECT TERMS (Continue on reverse if necessary and identify by block number)	
FIELD	GROUP	SUB GR	
08	11	Rocket Plume Acoustics STS Seismic-Acoustic Fields	
20	01	Acoustic Coupling STS Launch Environment	
		Vibro Acoustics Kennedy Space Center	
19. ABSTRACT (Continue on reverse if necessary and identify by block number)			
<p>The dense watercloud produced by STS main engine firing attenuates surface pressure levels directly south of Pad 39A by as much as 14db. Spectra at stations under the cloud are lower in level and frequency content than those in the clear. The phase velocity for acoustics early in the launch is insensitive to watercloud effects for stations at 300 meters. Spatial coherence of the pressure field is degraded between stations 100 meters or more apart.</p>			
20. DISTRIBUTION/AVAILABILITY OF ABSTRACT UNCLASSIFIED/UNLIMITED <input checked="" type="checkbox"/> SAME AS RPT <input type="checkbox"/> DTIC USERS <input type="checkbox"/>		21. ABSTRACT SECURITY CLASSIFICATION UNCLASSIFIED	
22a. NAME OF RESPONSIBLE INDIVIDUAL Henry A. Ossing		22b. TELEPHONE NUMBER <i>(Include Area Code)</i> (617) 861-3222	22c. OFFICE SYMBOL AFGL/LW

TABLE OF CONTENTS

	Page
1.0 <u>INTRODUCTION</u>	3
1.1 Statement of Need	3
1.2 Purpose of Work	3
2.0 <u>FINDINGS</u>	5
3.0 <u>CONCLUSIONS</u>	7
4.0 <u>MEASUREMENT SYSTEM</u>	9
4.1 Sensor Locations	9
4.2 Channel Response	10
4.3 Measurement Error	10
4.3.1 Digitization Aliasing Error	10
4.3.2 Uncorrelated Additive Noise	11
5.0 <u>LAUNCH GENERATED SURFACE PRESSURE</u>	13
5.1 SRB Ignition	13
5.2 Plume Envelope	14
5.3 Temporal Aspects of Launch Spectra	15
5.4 Plume Spectra In Standard Form	15
5.5 Phase Velocity	16
5.6 Coherence	18
5.6.1 Coherency (Temporal)	18
5.6.2 Coherency (Spacial)	19
5.7 Watercloud Attenuation	19
5.8 Comparison To Other Data	21

6.0	<u>FLIGHT 41B (STS-11) LAUNCH ELEVATIONS</u>	23
7.0	<u>REFERENCES</u>	31
8.0	<u>ILLUSTRATIONS</u>	33
9.0	<u>APPENDICES</u>	
9.1	Appendix A, Channel Responses	57
9.2	Appendix B, Glossary	67
9.3	Appendix C, Measurements	69

Accession For	
NTIS GRA&I	<input checked="" type="checkbox"/>
DTIC TAB	<input type="checkbox"/>
Unannounced	<input type="checkbox"/>
Justification	
By _____	
Distribution/	
Availability Codes	
Dist	Avail and/or Special
A-1	

DTIC
COPY
INSPECTED
1

1.0 INTRODUCTION

1.1 Statement of Need - There is a need to measure and analyze the vibro-acoustic environment of Space Transportation System (STS) launches in order to forecast and verify facility design and lifetime predictions for STS operations at Vandenberg Air Force Base (VAFB), and to accumulate flight vehicle performance data.

1.2 Purpose of Work - Earlier measurements at Kennedy Space Center (KSC) by NASA (1) and Air Force Geophysics Laboratory (2) pointed to an azimuthal dependence in the overall sound power level (OASPL) for STS launches. The immediate aim of this effort is to clarify the azimuthal properties of surface pressure around the time of the OASPL maximum for KSC launches. The study helps define and locate a site insensitive STS source pressure equivalent essential to vibro-acoustic forecasts at VAFB.

The acoustic environment produced by rocket engine firings has been characteristically couched in terms of pressure level variation with distance and frequency. Additional information is needed to treat the vibro-acoustics of large class structures. As used here, a structure is large when its size exceeds the wavelength of the incident acoustics. Vibro-acoustic forecasts for large structures require that the phasing and coherence of the acoustic load also be specified. Sufficient data were not available to establish the level, phase and coherence of launch loads for vibro-acoustic forecasts of Ground Support System (GSS) elements at VAFB.

Data taken at KSC serve to describe the pressure field produced by a shuttle over relatively flat, uncluttered topography. These pressure

measurements, after correction for ground reflections and watercloud effects, allow definition of a site independent STS source pressure. This source term, when combined with site specific responses forms the basis for upgrading GSS vibro-acoustic forecasts for STS launches at VAFB.

2.0 FINDINGS FOR STS-41B

- OASPL maxima at 300 meters are azimuth sensitive.
- Surface pressure levels clear of the launch generated ground-cloud are in harmony with NASA observations and Air Force Geophysics Laboratory (AFGL) forecasts.
- The spatial coherence of launch surface pressure becomes degraded between points separated by as much as 100 meters at an average range of 300 meters.
- Pressure spectra with the shuttle near the ground have a higher frequency content than those with the rocket at altitude.

3.0 CONCLUSIONS

- STS main engine firing at KSC produces a dense watercloud directly south of the launch mount that affects surface sound pressure level (SPL) well after liftoff. Peak levels under the cloud at 300 meters are attenuated 14 db or more for frequencies above 10 Hz. Below 5 Hz, SPL is largely uninfluenced by watercloud conditions.

- Acoustic velocities for stations in the clear are the same as those found earlier using observations under the cloud. Propagation through the cloud does not materially affect average phase. Quite likely, it introduces a random element into pressure measurements that degrades spatial coherence.

4.0 MEASUREMENT SYSTEM

Measurement System - The AFGL Geokinetic Data Acquisition System (GDAS) used in this effort collects, displays, stores and analyzes geophysical observations. As configured here, Figure 1, the unit accepts the output of 16 pressure sensors. Each sensor output is converted into a 12 bit binary word at the rate of 100 conversions per second. These data are then merged with identification, error suppression, time and status codes before storage on tape with back-up dump to bubble memory. Bubble memory was used as the system and back-up device because of its high immunity to vibration.

Measurements were initiated off-site from the Launch Control Center (LCC) 3 minutes prior to lift-off (T=0) and continued to T+15 minutes.

4.1 Sensor Locations - Pressure sensors were located on the ground surface over an arc 300 meters west and south of pad 39A, Figure 2. Observations over this arc are subject to a wide range in exhaust duct watercloud conditions. Sensors directly south of the pad reoccupy points previously used for Mission 5 (2). Observations at this azimuth are blanketed by a watercloud prior to Solid Rocket Booster (SRB) ignition. In contrast, sensors to the northwest (Stations 1 thru 3) are clear of an intervening cloud over most of the launch.

The bulk of the observations were taken along a radial southwest of the launch mount. Measurements within a small array at 300 meters along this radial are used to define the spatial attributes of the pressure field 200 to 400 meters from the launch pad.

A sensor pair at the center of the array is essentially collocated for acoustic phenomena of less than 50 Hz. These sensors are used to

isolate and estimate an independent additive noise term arising from turbulence and hardware sources.

4.2 Channel Response - Channel scale factors were measured at KSC just prior and subsequent to Flight 41-B . Known pressure and electrical transients inserted into the system determine individual channel scale factors and GDAS response characteristics. The bandpass used reflects the poor signal to noise ratio (S/N) inherent to low frequency measurements of rocket signals (3) corrupted by wind noise (4) and the important eigen-frequencies of major (GSS) elements at VAFB (5).

Table 1 summarizes GDAS response before and after launch. No significant shift occurred in the system's measurement characteristics across the launch. The calibrations have an overall repeatability of about 1% at a 1 sigma level.

4.3 Measurement Error - Two measures of data fidelity are considered. One depends on launch generated acoustics; the other relates to voltage fluctuations due to turbulence and hardware noise sources.

It is worth noting that acoustic measurements over a significantly larger bandwidth than reported here must envision not only higher sample rates, but larger word size. Also, considerably more attention should be given to sensor idiosyncracies, signal conditioning and additive noise. For our limited problem, the vibro-acoustics of large structures 100 meters or more from a STS launch, the band of interest is amply covered by GDAS, as presently configured.

4.3.1 Digitization Aliasing Error - The overall response of Channel 1 satisfying component values given in Appendix A is shown to

twice the Nyquist frequency, $f_N=50$ Hz, Figure 3. Protection ratios (6) defined by the amplitude ratio of the expected rocket signal in the measurement passband to the corresponding firstfold value of that frequency are given in Figure 4. For the conditions of our measurements, aliasing errors are negligible for frequencies less than 30 Hz.

4.3.2 Uncorrelated Additive Noise - We calculate the uncorrelated, additive noise due to wind turbulence and hardware sources at launch time from coherency estimates between sensor pair (8,9) separated by 1 meter. For acoustic inputs of less than 50 Hz, the sensors are sufficiently close to be considered common. In contrast, voltage fluctuations excited by small, slow moving eddies and internal hardware noise sources are largely uncorrelated both between channels and with the acoustic load produced by the propulsion system.

Figure 5 is our S/N estimate based on 10 data segments starting 8.0 seconds after SRB ignition. The S/N value obtained is the ratio of the square root of the coherent and incoherent spectra between channels (8,9). Stable S/N estimates can be obtained by ensemble averaging over a sample set as small as this when coherencies are as high as those encountered here (7).

Estimates of hardware noise free from turbulence were also made on GDAS a few days prior to launch with the pressure transducers clustered in stagnant air on the optics bench inside the Azimuth Alignment Tunnel (J8-1858), Figure 2. The uncorrelated noise between channels for this test, Figure 6, approaches the theoretical quantization and resistive noise for GDAS. Comparison between these noise spectra and noise residuals encountered during launch show our pressure measurements to be environmentally noise limited.

5.0 LAUNCH GENERATED SURFACE PRESSURE

Pressure time histories following main engine ignition are shown in Figure 7 for stations spread nearly uniformly over an arc of 180°. Launch generated surface pressure at 300 meters is azimuth dependent. The affect of station orientation moderates with time as the Shuttle clears the launch pad except for measurements directly under the exhaust duct groundcloud.

5.1 SRB Ignition - SRB ignition produces a conspicuous pressure transient at Stations 1 through 3, northwest of the pad. The ignition transient at this heading is an order of magnitude larger than those measured elsewhere both for observations in the clear, as at Stations 4, 10 and 16, or for observations blanketed by the watercloud, as at Stations 13, 14 and 15.

Observations taken at Stations 6-11 just after SRB ignition are used to predict surface pressure 100 meters toward and away from the launch mount. Figure 8 is the phase velocity calculated for the ignition wavelet over this station set. The ignition wavelet propagates outward from the launch mount at a median velocity, $C=342$ meters/second, independent of frequency. Pressure within the array area at a range R_0 and time t , are extrapolated radially to a range R by:

$$p(R,t) = \frac{R_0}{R} p(R_0, t + (R-R_0)/C)$$

with $C = \omega/k = 342$ meters/sec.

Figure 9 presents the observed, predicted and difference pressures for Stations 5 and 12 respectively for acoustics emanating from the launch

pad shortly after SRB ignition. The residuals are small in the prediction interval. Surface pressure at this range can be extrapolated radially using 1/R spreading and an acoustic velocity in harmony with the temperature and wind conditions prevailing at launch time. Such pressures are by definition spatially coherent.

5.2 Plume Envelope - Rocket launch pressure time histories measured by fixed ground stations are transient events. We describe the temporal properties of the launch pressure envelope encountered at KSC by calculating the SPL within a sliding data gate of T seconds duration starting at time t.

$$\text{SPL} (t, r) = \left\{ \langle (p(t) - \bar{p})^2 \rangle_T \right\}^{1/2}$$

Figure 10 is the SPL in our measurement passband for a 1.0 second data gate starting at time t, at each of the 16 stations. Plume envelope characteristics are azimuth dependent. Table 2 summarizes the time and magnitude of the SPL maxima for 1 second averages compensated to a common distance of 300 meters by 1/R scaling. The surface maxima at KSC are substantially weaker and later directly south of pad 39A. Broadband pressure levels measured here are dominated by watercloud effects for times well after liftoff with the shuttle in roll clear of the launch mount.

Plume pressure measurements at 320° free of intervening waterclouds attenuate as 1/R: Station pressures along a radial at 223°, partially covered by waterclouds, do not.

The median SPL maximum for 1 second averages referenced to 300 meters is 148 db.

5.3 Temporal Aspects of Launch Spectra - A sequence of spectra based on periodogram averaging (8) of overlapping 2.56 second data segments, measured 1 second apart at Stations 6-11 are given in Figures 11a through g. The first three spectra have the appearance of a high passed, independent, random process with a corner frequency at 6 Hz. The remaining spectra exhibit the bell-shape characteristic of undeflected rocket plumes. Spectra around the time of the OASPL maximum are in harmony with forecasted values (9). Following the peak, SPL decays in exponential fashion with a shift towards lower frequencies. Both the exponential decay and red shift have been noted for other rocket launches (9).

The load envelope for STS launch acoustics is frequency sensitive. For small stiff structures with major responses at 10 Hz or higher, important loads are azimuth sensitive and short lived. For large structures with responses at 10 Hz or less as at VAFB, the loads of concern are less influenced by site specific structures and are more persistent. Vibro-acoustic estimates based on broadband load duration will underestimate vibration levels caused by low mode, lightly damped responses of large structures.

5.4 Plume Spectra in Standard Form - After Hartnett (10), we construct stable broadband estimates of surface pressure spectra by fitting individual periodograms to the spectral form advocated by Powell (11) for undeflected, plume generated acoustics. The estimate:

$$G(f) = \frac{4}{\pi} \frac{OASPL}{f_m} \left\{ \frac{f}{f_m} + \frac{f_m}{f} \right\}^{-2}$$

establishes values of OASPL and the frequency at the spectral maximum,

f_m , that minimizes the square of the residuals between periodogram coefficients and $G_{pp}(f)$. The least squares estimate for a pressure sample from Station 6 starting 11 seconds after lift-off is shown in Figure 12.

Two tests are run to confirm when surface pressure can be represented by a random process of the spectral form $G_{pp}(f)$. One test is given in Figure 13. The figure plots the observed residuals against the distribution of a Chi squared variate with two degrees of freedom (DOF) the expected distribution, had we fitted periodogram ordinates to the true process (12). The plot is constructed to make validation one of simply accepting when the residuals lie on the indicated straight line. Through this test and one based on a figure of merit established by simulation, we find surface pressure is well represented by spectra of the form $G_{pp}(f)$ for data samples starting 9 seconds or more after lift-off. For earlier times, periodograms do not satisfy the form ascribed to an undeflected plume, and rightly so.

Table 3 lists OASPL and f_m values that best fit our measurements for times shortly after lift-off. The maximum OASPL for 2.56 second averages at 300 meters occurs 11 seconds after lift-off for measurements at a heading of 225°. The array median OASPL value is 148 db. The spectrum is a maximum at 7.4 Hz.

5.5 Phase Velocity - The pressure, $p(R,t)$ caused by acoustics propagating outward from a small source located at the origin of a windless, isothermal, unbounded atmosphere is completely coherent along any radial segment with an amplitude and phase determined from its Fourier transform.

$$p(R, \omega) = p(\omega) \cdot \frac{1}{R} \exp i \left\{ kR + \phi_s \right\}$$

$$k = \omega / C_a$$

with C_a , the speed of sound in air, and ϕ_s the phase at the source. In contrast, pressure fields caused by distributed, independent sources invariably lead to incoherent fields for separated observers. Further, the magnitude of the coherence loss generally increases with separation.

Pressure measurements, $p(r_\ell, t)$ at pad distances r_ℓ , $\ell = 1, 2, \dots, L$ and time t , are taken to be spatially coherent far field acoustics corrupted by additive noise. Under this representation the magnitude of the ratio of k weighted vector and scalar sums of $p(r, \omega)$

$$v(k, \omega) = \left| \frac{\sum_{\ell=1}^L p(r_\ell, \omega) e^{ikr_\ell}}{\sum_{\ell=1}^L |p(r_\ell, \omega)|} \right|$$

approaches unity for large S/N measurements with $C = \omega/k$.

Figure 14 plots the absolute maxima of $v(k, \omega)$ of k weighted Fourier coefficients for 2.56 second samples starting just prior to SRB ignition. In the band where ignition pressure is large, Figure 15, the magnitude of $v(k, \omega)$ is close to unity. Measured pressures are coherent under a phase shift given by $kr_\ell = \omega r_p$ for Stations 6 through 11.

Figure 16 locates (k, ω) pairs for absolute maxima $v(k, \omega)$ values for the same SRB ignition sample. The plot establishes the propagation characteristics for surface pressure shortly after ignition. The phase velocity, C , calculated directly from ω/k ratios is given in Figure 8. The median C value in the band $.39 \leq f \leq 25$ Hz is 342 meters/second. For these frequencies, launch generated surface pressure is well represented as a coherent, non-dispersive, acoustic disturbance propagating outward from a single small source region located near the launch pad.

Figure 17 summarizes velocity estimates determined in like manner from (k, ω) pairs over a sequence of pressure samples from Stations 6 through 11. The measured surface pressures are well represented by acoustics emanating from a small source that rises over the launch mount. Phase velocities obtained here closely match earlier velocity estimates (2) that use measurements taken directly south of the launch mount, under the watercloud. Refraction in the watercloud does not appear to be an important factor.

5.6 Coherence

5.6.1 Coherency (Temporal) - Ordinary coherence defined through cross and auto-spectra of sequences obtained between station pair (a,b) measures the amplitude-phase stability of data sets over time. For a constant amplitude-phase relation, coherency is unity. For a purely random amplitude-phase relation, longtime estimates of coherency approach zero.

$$0 \leq \langle \gamma_{ab}^2(f) \rangle_T = \frac{|G_{ab}(f)|^2}{G_a(f) \cdot G_b(f)} \leq 1$$

The coherence of acoustics emanating from a simple monopole moving in space, measured at fixed locations, is always less than unity when the difference distance between source-station pairs changes with time. Ordinary estimates of coherency based on time averaged pressure measurements, uncompensated for source motion, are low in value and of limited utility shortly after the rocket leaves the pad. Figure 18 is an estimate of ordinary coherency based on 6 data sets from station pair (6,12) starting at 08:00:00.5 and ending at 08:00:14.6. Over this time interval, Shuttle motion degrades ordinary coherency estimates. Coherence loss over time is a common feature for close-in launch pressure measurements (9).

5.6.2 Coherency (Spatial) - Rather than determining the ratio of the magnitude of vector and scalar averages between a pair of points over time, as is done in ordinary coherence, we average spatially. In harmony with temporal estimates, we define spatial coherence by the square of the ratio:

$$\gamma^2(k, \omega) = \left| \frac{\sum_{\ell=1}^L p(r_{\ell}, \omega) e^{ikr_{\ell}}}{\sum_{\ell=1}^L |p(r_{\ell}, \omega)|} \right|^2$$

with k equal to (ω/c) .

Figure 19 is an estimate of $\gamma^2(k, \omega)$ based on 2.56 second pressure samples from Stations 6,7,8,10,11 starting 10.8 seconds after launch. The spatial coherency over this station set is almost unity; pressure at this time over an area this size is well represented by acoustics coming from a point 100 meters below the rocket, 200 meters above the launch mount.

Estimates of $\gamma^2(k, \omega)$ also based on five 2.56 second pressure samples starting at 10.8 seconds over a much larger area are given in Figure 20. Spatial coherency for stations separated by as much as 100 meters is less than unity. For an area as large as this, about 75% of the launch pressure can be represented by acoustics propagating outward from a small source located over the launch mount.

5.7 Watercloud Attenuation - Attenuation due to the watercloud is estimated around the time of the SPL maxima by contrasting measurements taken in the clear with those found under the cloud. Table 4 summarizes standard form spectral parameters for acoustics that share a common source time but different cloud conditions.

TABLE 4

Ch#	<u>Az</u> (deg)	<u>f_m</u> (Hz)	<u>T</u> (sec)	<u>OASPL</u> (psi ² /sec)	<u>OASPL</u> (psi ² /sec) re:300m
1	320°	15.3	7.50	6.17 10 ⁻³	9.18 10 ⁻³
2	320°	10.9	7.20	10.00 10 ⁻³	7.20 10 ⁻³
14	180°	4.1	7.31	0.30 10 ⁻³	0.28 10 ⁻³
16	145°	9.2	7.32	3.12 10 ⁻³	2.91 10 ⁻³

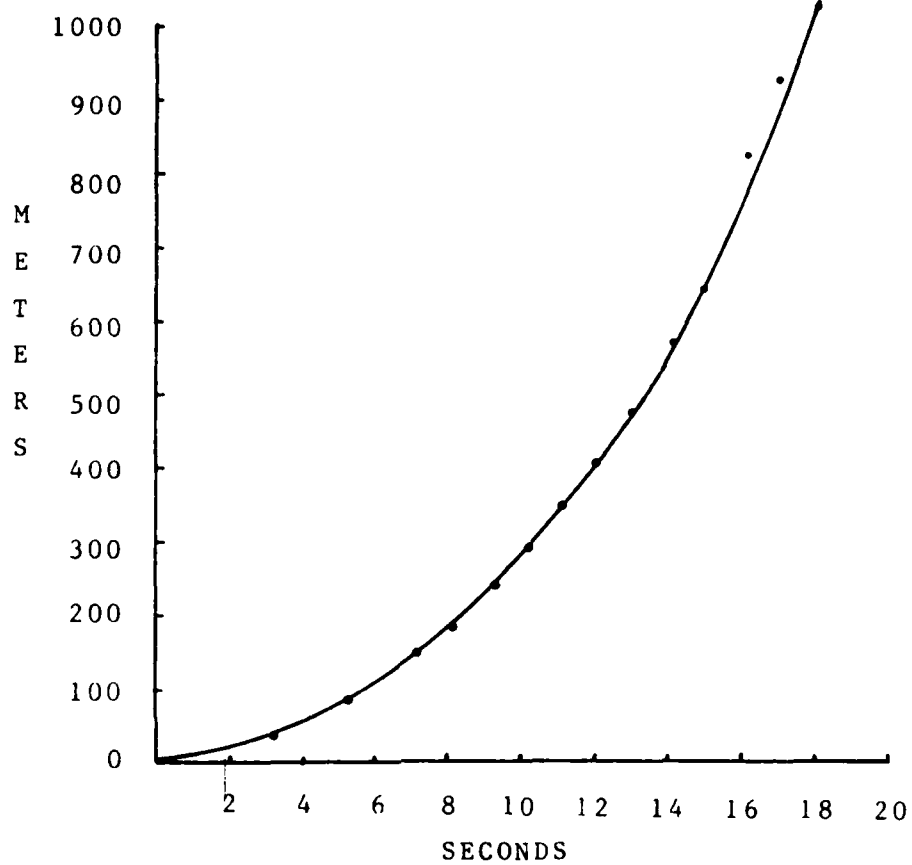
Figure 21 is the square root of the ratio of the standard spectra obtained at Station 14 under the watercloud with that from Station 2 taken in the clear, compensated to a common distance of 300 meters. The result is attenuation due to the watercloud when the stations share a common source term.

The lowpass characteristic found for the watercloud path is intuitively reasonable. Further, persistent low pressure levels under the cloud with the Shuttle in roll above the pad argue that the major cause for low pressure levels south of 39A is watercloud attenuation, not source asymmetry once the Shuttle clears the launch mount.

5.8 Comparison to Other Data - OASPL maxima for STS-5 at 180° measured by GDAS were unexpectedly low (2). The present effort seeks to resolve the cause of the discrepancy between these measurements and levels reported earlier by NASA. We find the disparity is due to gross differences in launch surface pressure with azimuth, not measurement error or flight nuances. Figure 22 gives SPL maxima for Mission 11 taken by GDAS at Station 1, 1200 feet from the pad at an azimuth of 320° as it relates to averaging time. Superimposed on the plot are SPL maxima reported by NASA for the same launch and station location (13). The reported values from these two sources agree to within 1 db.

Standard form spectral parameters for STS-5 and STS-11 are contrasted in Table 5 for a common station 290 meters from the launch point at a heading of 180°. Maximum OASPL estimates repeat to within a few db. Estimates of the spectral maximum and its location across the two launches differ somewhat more. Data scatter between launches at the 180° heading may well be greater than scatter at stations in the clear, for measurements under the watercloud must also include cloud vagaries due in part to meteorologic conditions at launch time.

6.0 FLIGHT 41B (STS-11) LAUNCH ELEVATIONS



Title STS-11 034-17
Flight Test STS-11
Test Date 03 FEB 84
Subsystem DYER NAV,GD,FC,RM
Meas. ID V95H0175C
Nomenclature CURR ORB ALT ABOVE REF ELLIPSOID

GDAS CALIBRATIONS, STS 41B

Ch	Pre Launch <u>1 Feb 1984</u>			Post Launch <u>3 Feb 1984</u>		
	f_{ℓ} (Hz)	G	f_h (Hz)	f_{ℓ} (Hz)	G	f_h (Hz)
1	.032	20.83	30.6	.035	20.69	30.5
2	.031	19.04	31.4	.034	18.84	31.3
3	.033	20.60	30.6	.032	20.46	30.6
4	.028	20.09	30.6	.032	19.48	30.6
5	.034	20.86	31.0	.036	20.66	31.1
6	.027	19.54	30.5	.030	19.41	30.6
7	.032	19.44	30.8	.034	19.31	30.8
8	.031	19.91	31.4	.036	19.80	31.4
9	.033	21.33	30.2	.036	21.09	30.2
10	.028	19.68	30.4	.033	19.50	30.4
11	.033	19.93	30.0	.035	19.75	29.9
12	.028	19.80	29.8	.033	19.61	29.9
13	.033	21.45	30.3	.032	21.27	30.3
14	.030	23.67	30.9	.035	25.52	30.9
15	.032	21.12	30.7	.034	20.97	30.8
16	.028	19.26	30.3	.034	19.10	30.1

f_{ℓ} low frequenc cutoff
 G midband gain, volts/psi
 f_h high frequency cutoff

TABLE 1

SPL MAXIMA, 1 SECOND AVERAGE

<u>Ch</u>	<u>Observed Max (psi)</u>	<u>Time of Maximum (sec)</u>	<u>Az (Deg)</u>	<u>Scale Distances (300 meters)</u>	<u>SPL Max (re:300 m) db</u>
1	.0569	9.3	320	1.22	147.5
2	.0827	8.5	320	.85	147.7
3	.1187	8.3	320	.61	147.9
4	.0761	9.0	248	.97	148.1
5	.0562	9.7	223	.69	142.6
6	.0690	10.9	223	.97	147.3
7	.0704	10.9	223	.99	147.7
8	.0720	10.9	223	.99	147.8
9	.0710	10.9	223	.99	147.7
10	.0674	10.9	223	.99	147.3
11	.0701	10.9	223	1.01	147.8
12	.0755	11.2	223	1.30	150.6
13	.0284	14.2	180	.94	139.4
14	.0352	14.2	180	.96	141.4
15	.0253	14.2	180	1.24	140.6
16	.0577	9.3	142	.97	145.7

TABLE 2

STANDARD SPECTRA FACTORS

Ch	T Sec	f _m Hz	SPL (25) Psi ² /Sec	OASPL Psi ² /Sec	M	Az Deg	r Ft	OASPL re: 300m Psi ² /Sec
1	8.0	11.4	2.15-03	4.24-03	1.35	320	1200	6.31*10 ⁻³
2	7.2	10.9	5.08-03	1.00-02	3.19	320	835	7.20*10 ⁻³
2	9.6	4.99	3.26-03	4.31-03	0.86	320	835	3.10*10 ⁻³
2	11.0	4.32	2.21-03	2.86-03	0.86	320	835	2.06*10 ⁻³
2	12.0	3.27	7.66-04	8.15-04	1.95	320	835	5.87*10 ⁻⁴
2	14.0	1.98	7.19-05	8.00-05	0.91	320	835	5.76*10 ⁻⁵
2	17.0	1.12	5.49-06	6.71-06	0.53	320	835	4.83*10 ⁻⁶
2	20.0	0.97	2.88-06	3.12-06	0.85	320	835	2.25*10 ⁻⁶
3	7.0	13.6	1.07-02	2.49-02	0.81	320	600	9.26*10 ⁻³
4	7.7	22.4	3.73-03	1.56-02	19.7	250	950	1.45*10 ⁻²
4	9.6	8.80	4.31-03	6.72-03	3.40	250	950	6.26*10 ⁻³
4	10.3	6.28	3.29-03	4.47-03	0.98	250	950	4.17*10 ⁻³
4	11.0	5.22	2.49-03	3.28-03	1.09	250	950	3.06*10 ⁻³
4	12.0	4.02	1.27-03	1.54-03	1.21	250	950	1.44*10 ⁻³
4	12.9	3.70	8.38-04	1.03-03	1.24	250	950	9.60*10 ⁻⁴
4	14.0	2.56	3.92-04	5.15-04	0.83	250	950	4.80*10 ⁻⁴
4	17.0	2.42	5.00-05	6.09-05	0.68	250	950	5.68*10 ⁻⁵
4	20.0	2.10	1.42-05	1.79-05	0.43	250	950	1.67*10 ⁻⁵
5	8.4	7.63	2.29-03	3.38-03	1.78	225	675	1.59*10 ⁻³
6	9.6	6.85	3.42-03	4.77-03	2.14	225	955	4.49*10 ⁻³
6	10.3	5.85	3.05-03	4.13-03	1.52	225	955	3.89*10 ⁻³
6	11.0	5.39	2.83-03	3.88-03	0.90	225	955	3.65*10 ⁻³
6	12.0	4.19	1.61-03	2.11-03	1.05	225	955	1.99*10 ⁻³

TABLE 3

STANDARD SPECTRA FACTORS

$\frac{C_n}{m}$	$\frac{T}{Sec}$	$\frac{f_m}{Hz}$	$\frac{SPL(25)}{Psi./Sec}$	$\frac{OASPL}{Psi./Sec}$	$\frac{M}{}$	$\frac{Az}{Deg}$	$\frac{r}{ft}$	$\frac{OASPL}{Psi./Sec}$ re: 300m
6	12.9	3.95	1.12-03	1.43-03	1.11	225	955	1.35×10^{-3}
6	14.0	3.00	4.23-04	6.43-04	0.81	225	955	6.06×10^{-4}
6	17.0	2.94	1.08-04	1.27-04	0.83	225	955	1.20×10^{-4}
6	20.0	2.79	2.82-05	3.35-05	1.03	225	955	3.16×10^{-5}
7	9.6	7.46	3.53-03	5.15-03	1.89	225	975	5.06×10^{-3}
8	9.6	7.30	3.59-03	5.20-03	1.88	225	975	5.11×10^{-3}
9	9.6	7.61	3.52-03	5.17-03	1.85	225	975	5.08×10^{-3}
10	9.6	6.85	3.14-03	4.45-03	1.86	225	975	4.37×10^{-3}
11	9.6	7.44	3.64-03	5.01-03	2.28	225	995	5.12×10^{-3}
12	9.9	9.26	3.08-03	5.50-03	0.80	225	1275	9.23×10^{-3}
13	12.9	3.30	6.03-04	9.54-04	0.89	180	925	8.43×10^{-4}
13	9.0	3.49	4.36-04	6.29-04	1.84	180	945	5.80×10^{-4}
14	9.6	3.44	5.33-04	7.95-04	0.94	180	945	7.33×10^{-4}
14	10.3	3.43	5.68-04	8.90-04	0.83	180	945	8.21×10^{-4}
14	11.0	3.41	7.31-04	1.15-03	0.78	180	945	1.06×10^{-3}
14	12.0	3.30	7.25-04	1.13-03	0.90	180	945	1.04×10^{-3}
14	12.9	3.30	9.16-04	1.44-03	0.85	180	945	1.33×10^{-3}
14	14.0	3.34	7.56-04	1.23-03	0.80	180	945	1.13×10^{-3}
14	17.0	2.75	1.40-04	1.99-04	0.69	180	945	1.84×10^{-4}
14	20.0	2.32	4.78-05	6.52-05	0.53	180	945	6.01×10^{-5}
15	12.9	3.77	5.14-04	7.97-04	0.70	180	1225	1.24×10^{-3}
16	8.0	11.9	2.20-03	4.41-03	11.3	140	950	4.11×10^{-3}
16	9.6	6.54	1.77-03	2.45-03	1.97	140	950	2.28×10^{-3}
16	10.3	4.63	1.01-03	1.36-03	0.74	140	950	1.27×10^{-3}

TABLE 3 (cont'd)

STANDARD SPECTRA FACTORS

<u>Ch</u>	<u>T</u> <u>Sec</u>	<u>f_m</u> <u>Hz</u>	<u>SPL(25)</u> <u>Psi²/Sec</u>	<u>OASPL</u> <u>Psi²/Sec</u>	<u>M</u>	<u>Az</u> <u>Deg</u>	<u>r</u> <u>ft</u>	<u>OASPL</u> <u>re: 300m</u> <u>Psi²/Sec</u>
16	11.0	3.65	6.61-04	0.40-04	0.54	140	950	8.76*10 ⁻⁴
16	12.0	3.04	3.86-04	5.28-04	0.76	140	950	4.92*10 ⁻⁴
16	14.0	3.46	4.78-04	6.37-04	1.01	140	950	5.94*10 ⁻⁴
16	17.0	3.57	1.60-04	1.71-04	2.93	140	950	1.59*10 ⁻⁴
16	20.0	2.63	6.03-05	6.53-05	1.94	140	950	6.09*10 ⁻⁵

TABLE 3 (cont'd)

TABLE 5

STS-5 & STS-11 SPECTRAL PROPERTIES

T Sec	OASPL		STS-5 f _m Hz	STS-11	G max	
	STS-5 db	STS-11			STS-5 psi ² /Hz	STS-11
9	139*	139	5.2*	3.5	4.2.10 ^{-5*}	5.7.10 ⁻⁵
11	139	141	4.4	3.4	5.1.10 ⁻⁵	1.1.10 ⁻⁴
14	137*	142	2.8*	3.3	5.1.10 ^{-5*}	1.2.10 ⁻⁴
17	132	134	2.5	2.8	1.9.10 ⁻⁵	2.3.10 ⁻⁵

* Periodogram does not satisfy distribution test for standard spectra.

TABLE 5

7.0 REFERENCES

- (1) NASA Report No. KSC-DD-457-TR, Space Shuttle STS 1 Launch Processed Ground Measurements, Vol. 1, (Sep 1981).

- (2) Crowley, F., Hartnett, E., Ossing H., Amplitude and Phase of Surface Pressure Produced by Space Transportation System - Mission 5, AFGL-TR-83-0039, (Jan 1983) ,ADA125-846.

- (3) NASA Report SP-8072, Acoustic Loads Generated by the Propulsion System, (1971).

- (4) Kimball, B and Lemon, E. Spectra of Air Pressure Fluctuations at the Soil Surface, J. Geophys. Res. 75; 6771-6777, (1970).

- (5) Yang, R. and Teegarden, W., Vibro-Acoustic Study, Martin Marietta Report VCR-79-145, (1980).

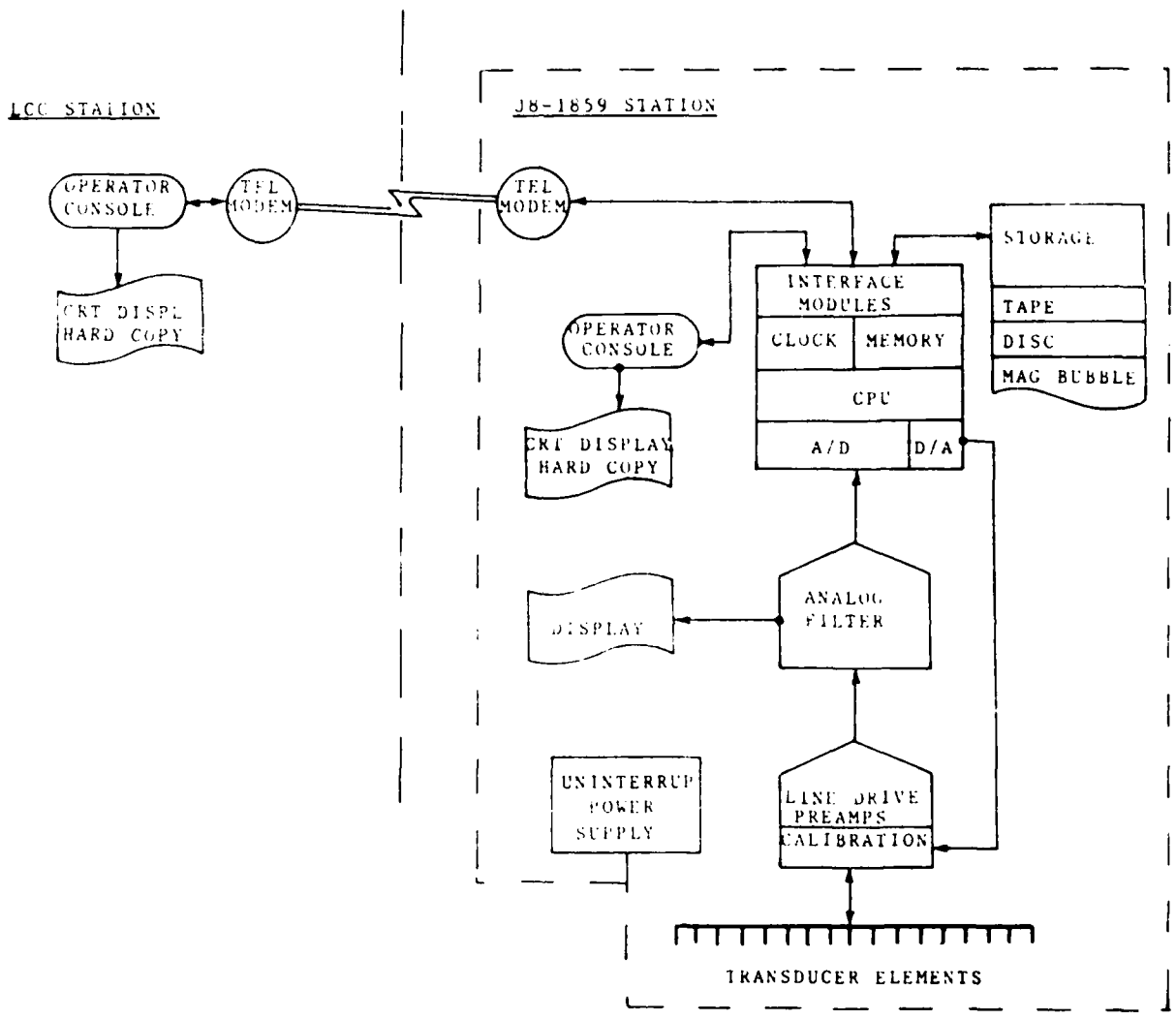
- (6) Blackman, R., and Tukey, W., The Measurement of Power Spectra, Dover Publications, New York, (1959).

- (7) Fay, J.W., Confidence Bounds for Signal-to-Noise Ratios from Magnitude Squared Coherence Estimates, IEEE Transactions on Acoustics, Speech and Signal Processing, Vol. ASSP-28, No. 6, DEC, (1980).

- (8) Oppenheim, A.V., and Schafer, R.W., Digital Signal Processing, Prentice-Hall Inc., (1975).
- (9) Crowley, F. et al., The Seismo-acoustic Disturbance Produced by a Titan III-D with application to the Space Transportation System Launch Environment at Vandenberg AFB, AFGL-TR-80-0358, (17 Nov 1980), ADA100209.
- (10) Hartnett, E. and Carleen, E., Characterization of Titan III-D Acoustic Spectra by Least Squares Fit to Theoretical Model, AFGL-TR-80-0004, ADA083021.
- (11) Powell, A., Theory of Vortex Sound, J. Acoust. Soc. Am., 36, 177-195, (1964).
- (12) Hinich, M.J., and Clay, C.S., The Application of the Discrete Fourier Transform in the Estimation of Power Spectra, Coherence and Bi Spectra of Geophysical Data, Reviews of Geophysics, Vol. 6, No. 3, (Aug 1968).
- (13) NASA Report No. KSC-DD-818-TR, Summary of Measurements of KSC Launch Induced Environmental Effects, (STS-1 through STS-11), (1984).

8.0 ILLUSTRATIONS

<u>Figure Title</u>	<u>Page</u>
1. GDAS Flight 41B	34
2. Sensor Locations, STS 41B	35
3. Channel 1 Response, STS 41B	36
4. Protection Ratios for Channel 2	37
5. Signal to Noise Estimate, STS 41B	38
6. Hardware Noise Estimate, Channel 2	39
7. Surface Pressure Time Histories	40
8. Phase Velocity for Ignition Wavelet	41
9. Pressure Extrapolation at Early Launch Times	42
10. Plume Pressure Envelope	43
11. Surface Pressure Spectra	44
12. Standard Form Spectra	46
13. Acceptance Test	47
14. $\gamma(k, \omega)$ Absolute Maxima	48
15. Ignition Wavelet Spectra	49
16. Measured Propagation Characteristics	50
17. Median Phase Velocities	51
18. Ordinary Coherency	52
19. Spatial Coherency: 10 meters	53
20. Spatial Coherency: 100 meters	54
21. Watercloud Attenuation Estimate	55
22. SPL Maxima	56

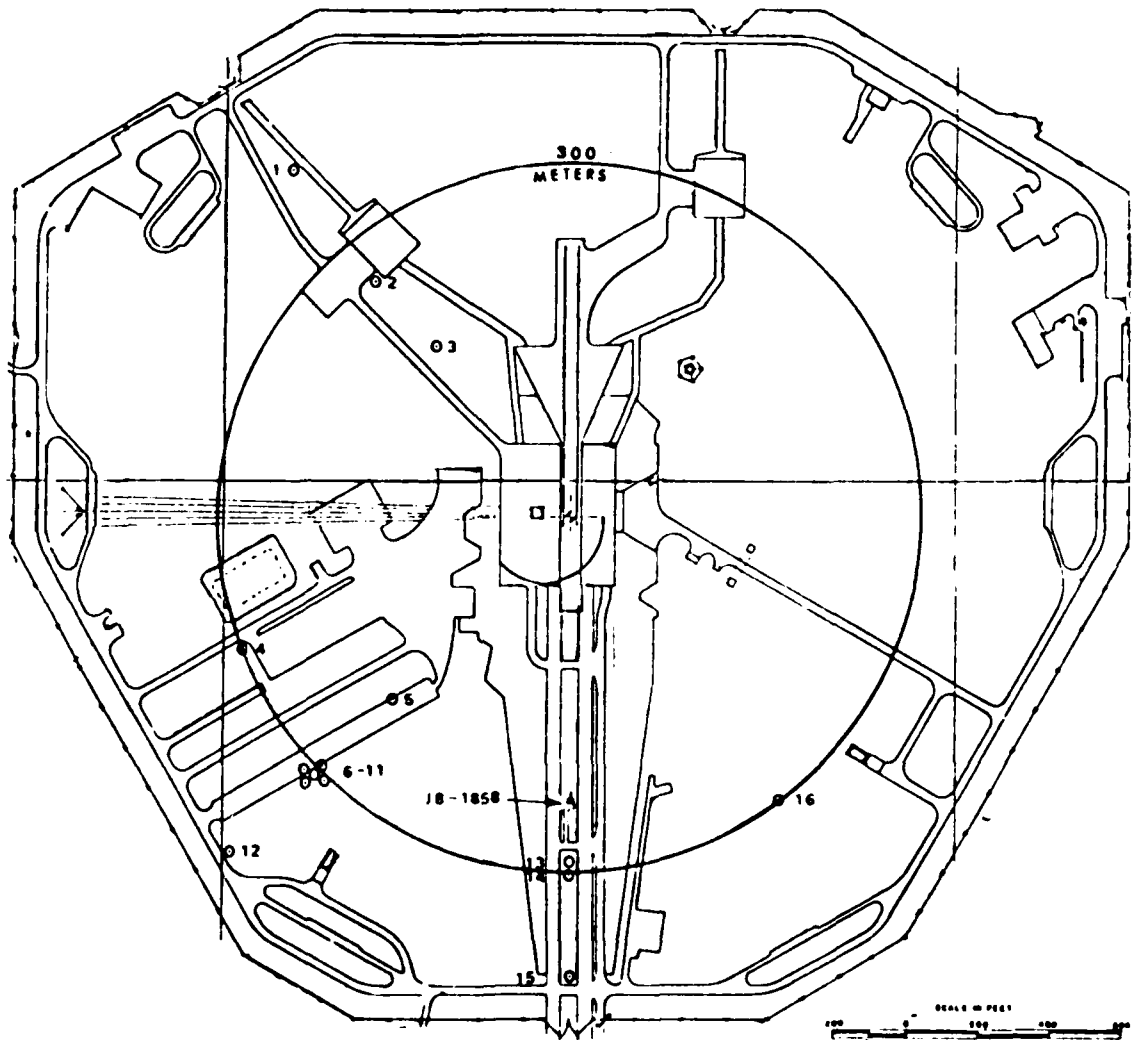


GDAS FLIGHT 41B

FIGURE 1

KSC PAD 39A

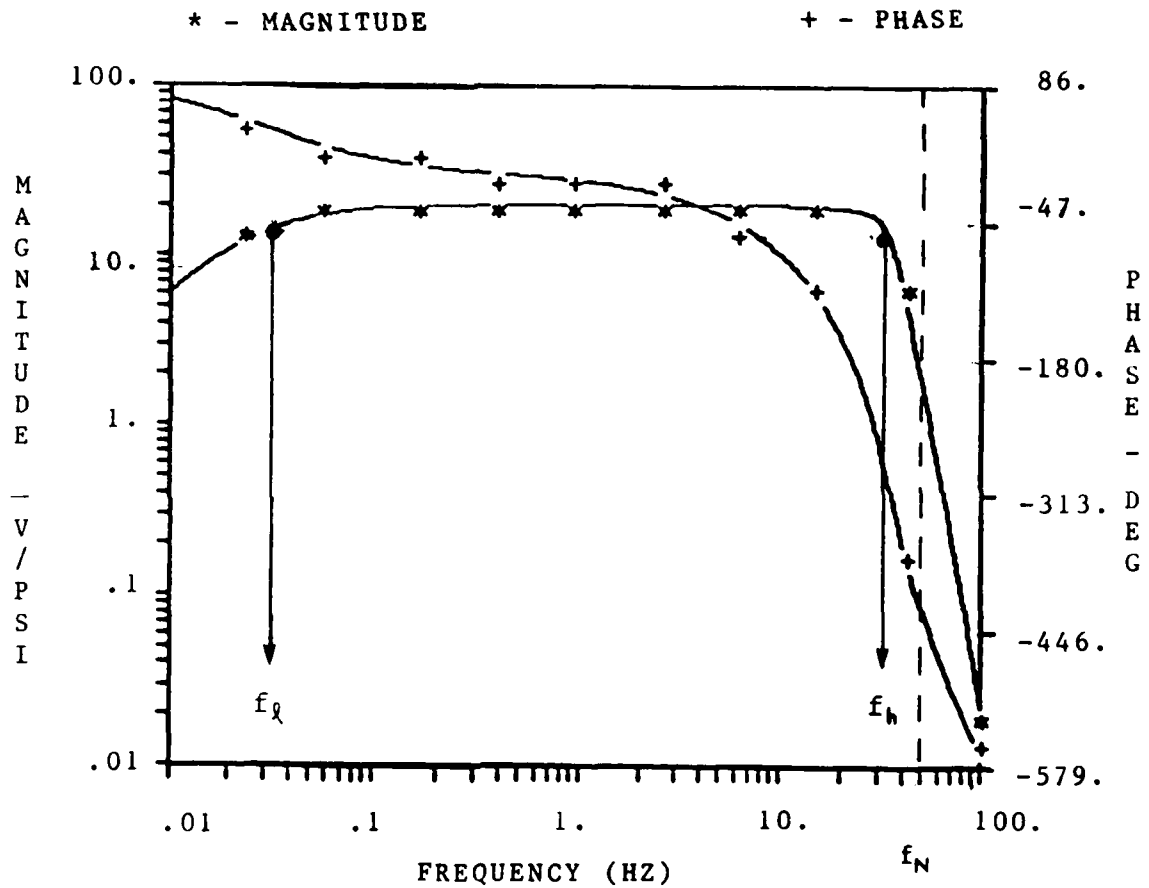
North



● Channel Number

SENSOR LOCATIONS, STS 41B

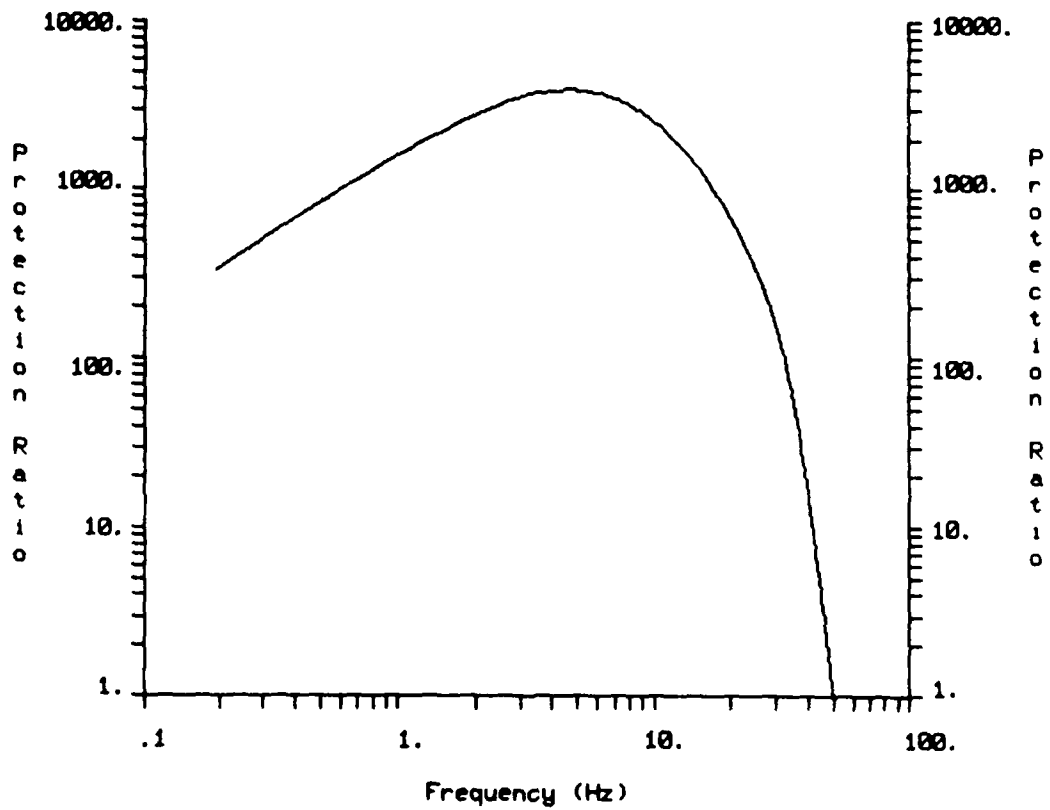
FIGURE 2



f_l low frequency cutoff
 f_h high frequency cutoff
 f_N Nyquist frequency

CHANNEL 1 RESPONSE, STS 41B

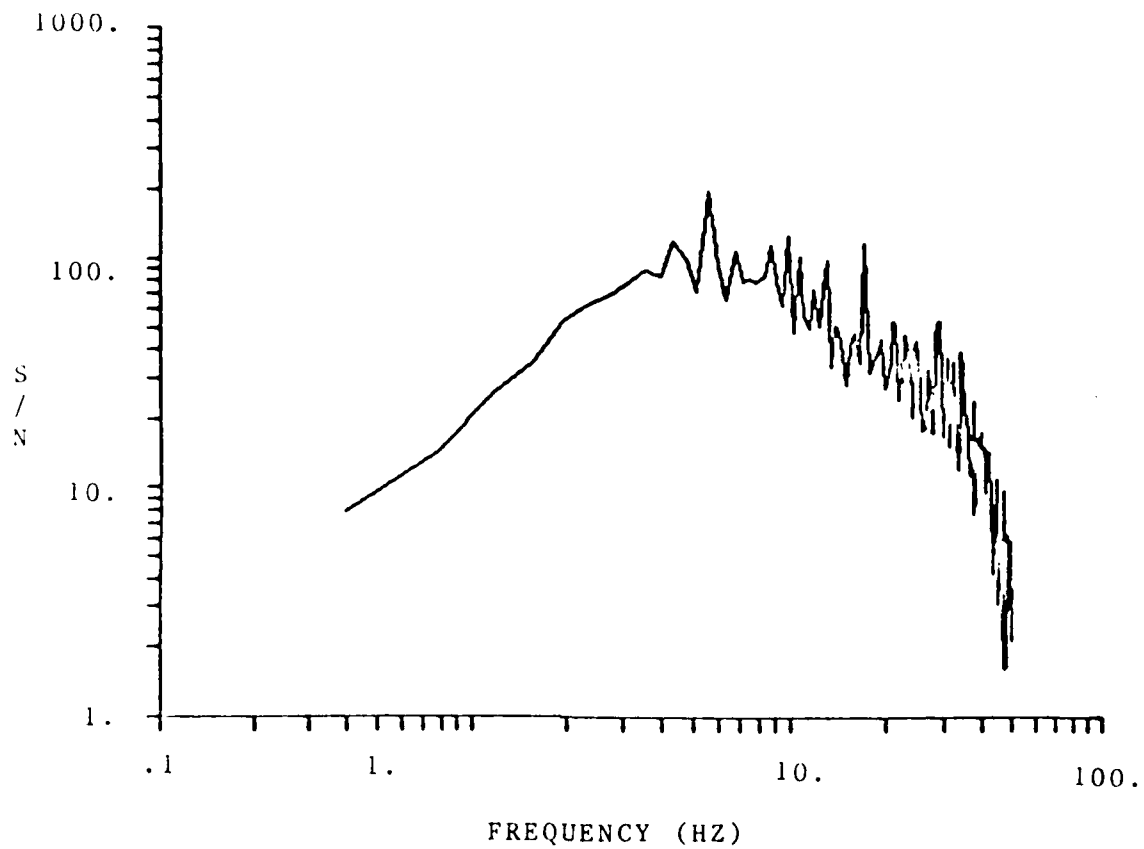
FIGURE 3



PROTECTION RATIOS FOR CHANNEL 2

FIGURE 4

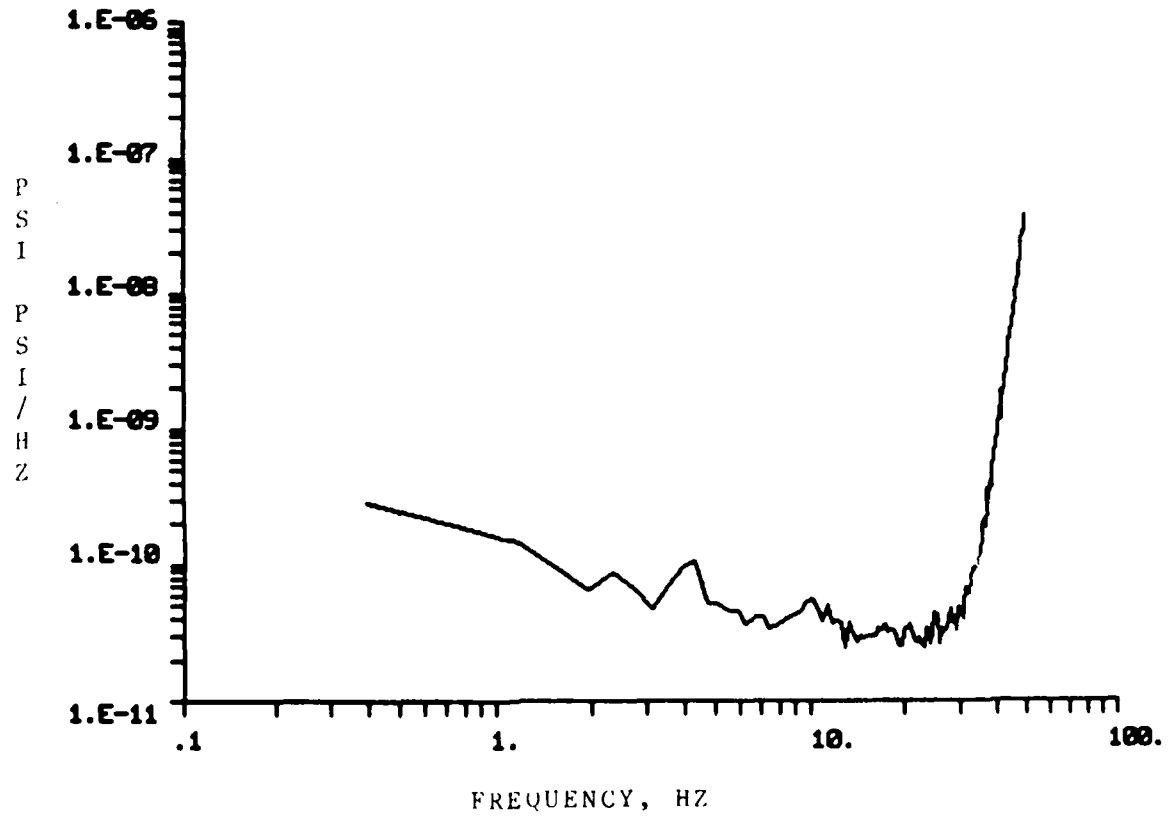
SIGNAL TO NOISE RATIO
20 DOF



SIGNAL TO NOISE ESTIMATE, STS 41B
KSC 3 FEBRUARY 1984

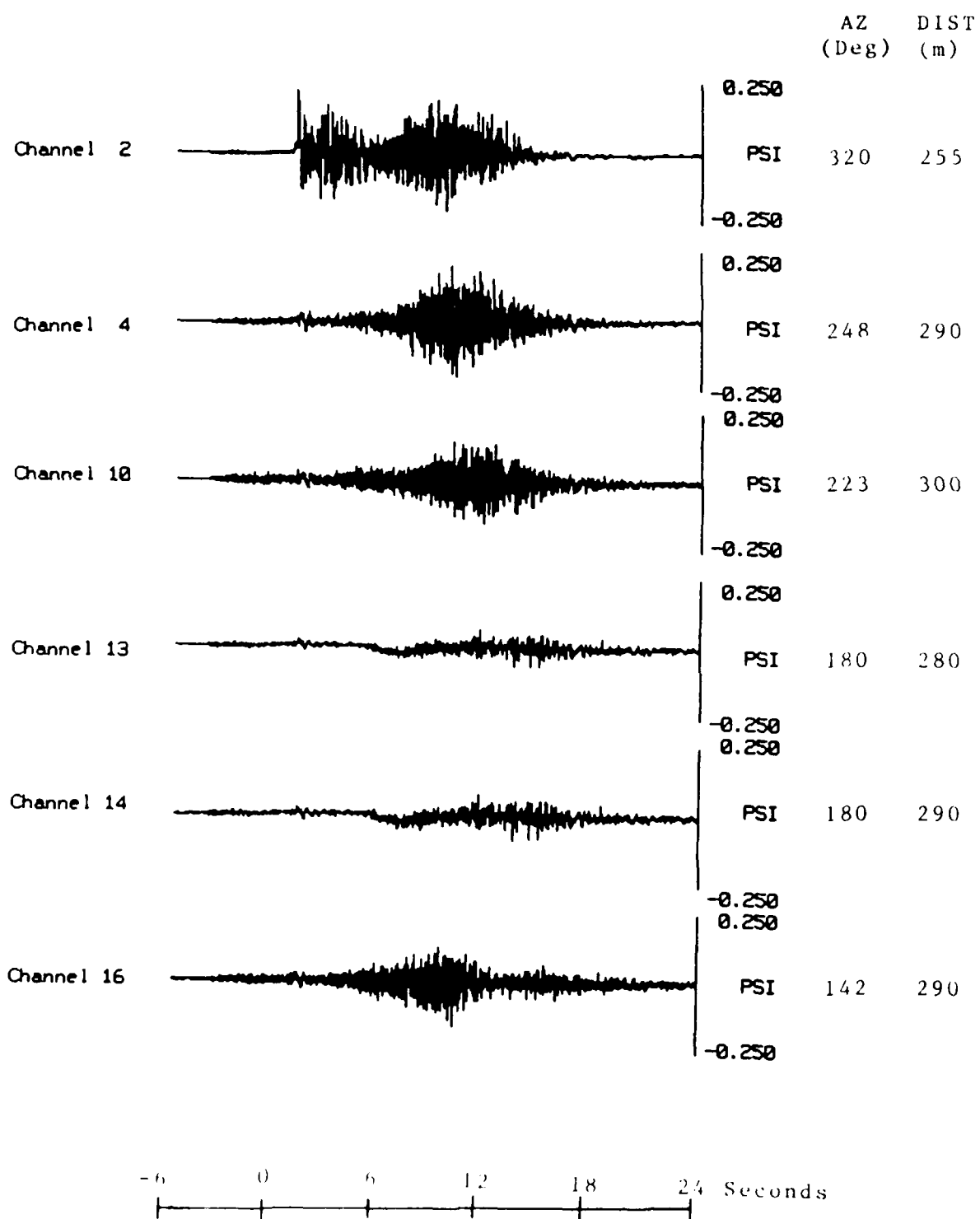
FIGURE 5

INCOHERENT PSD OF CHANNEL 2 96 DOF



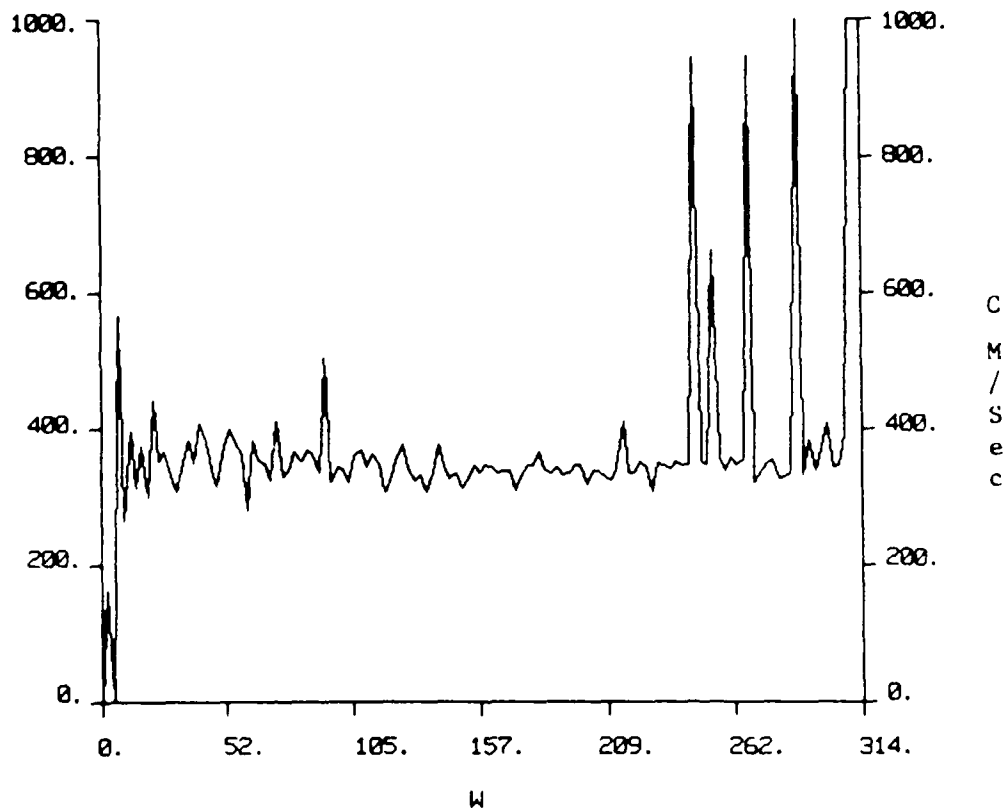
HARDWARE NOISE ESTIMATE, CHANNEL 2

FIGURE 6



SURFACE PRESSURE TIME HISTORIES

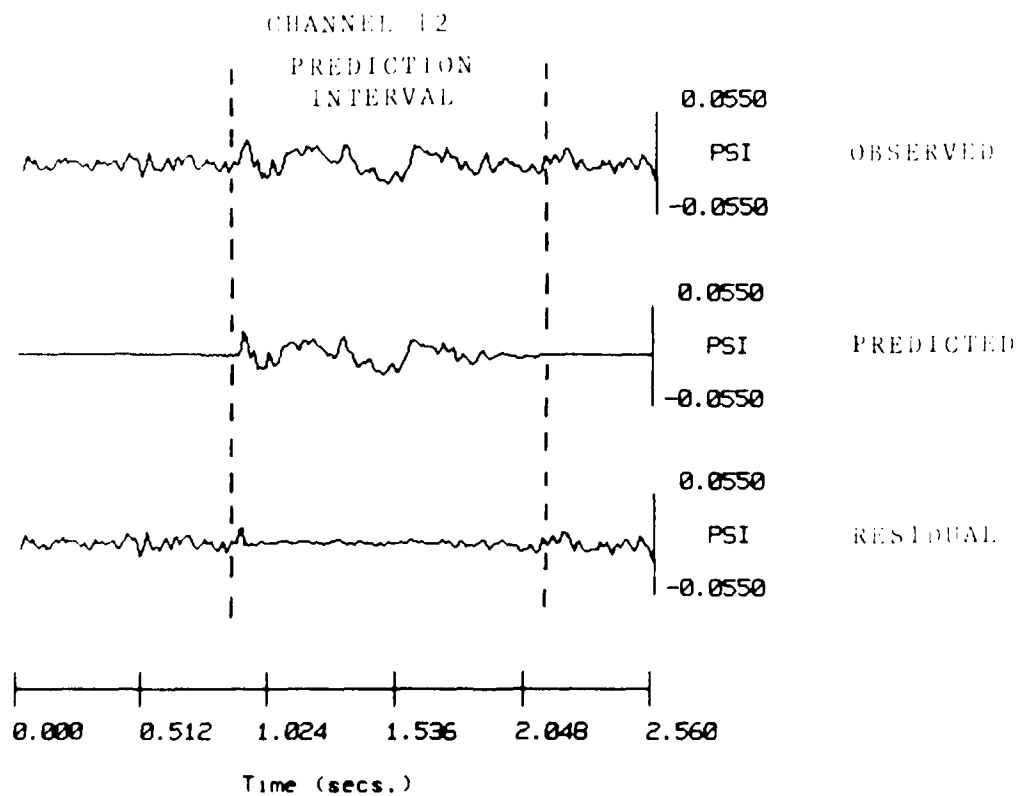
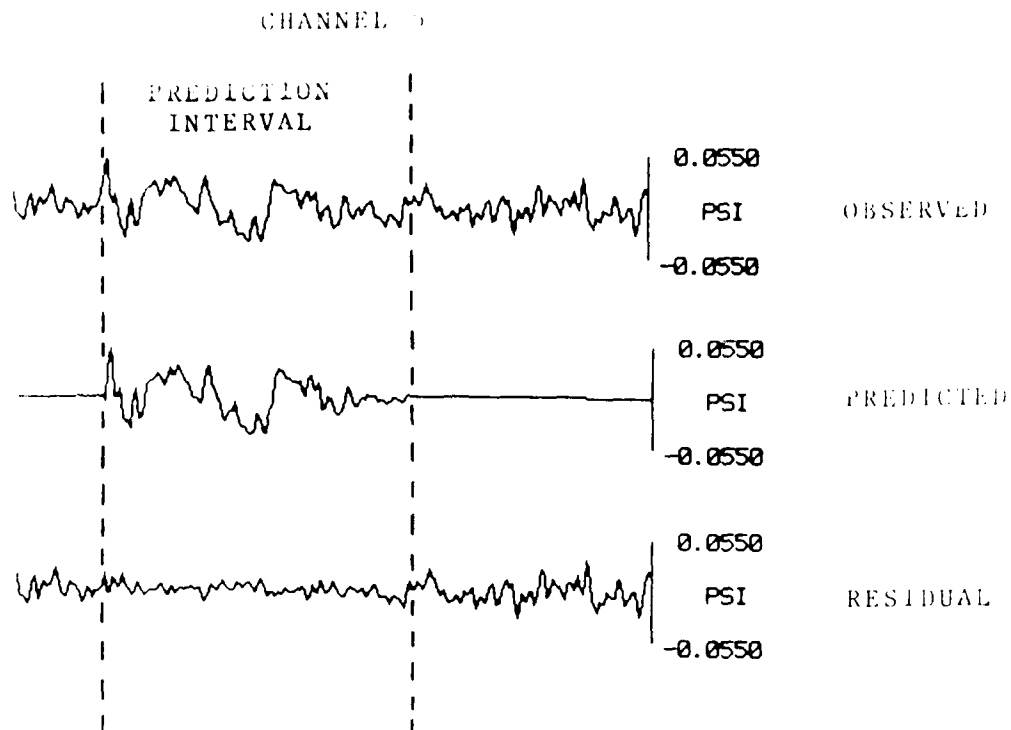
FIGURE 7



Median = 341.9397

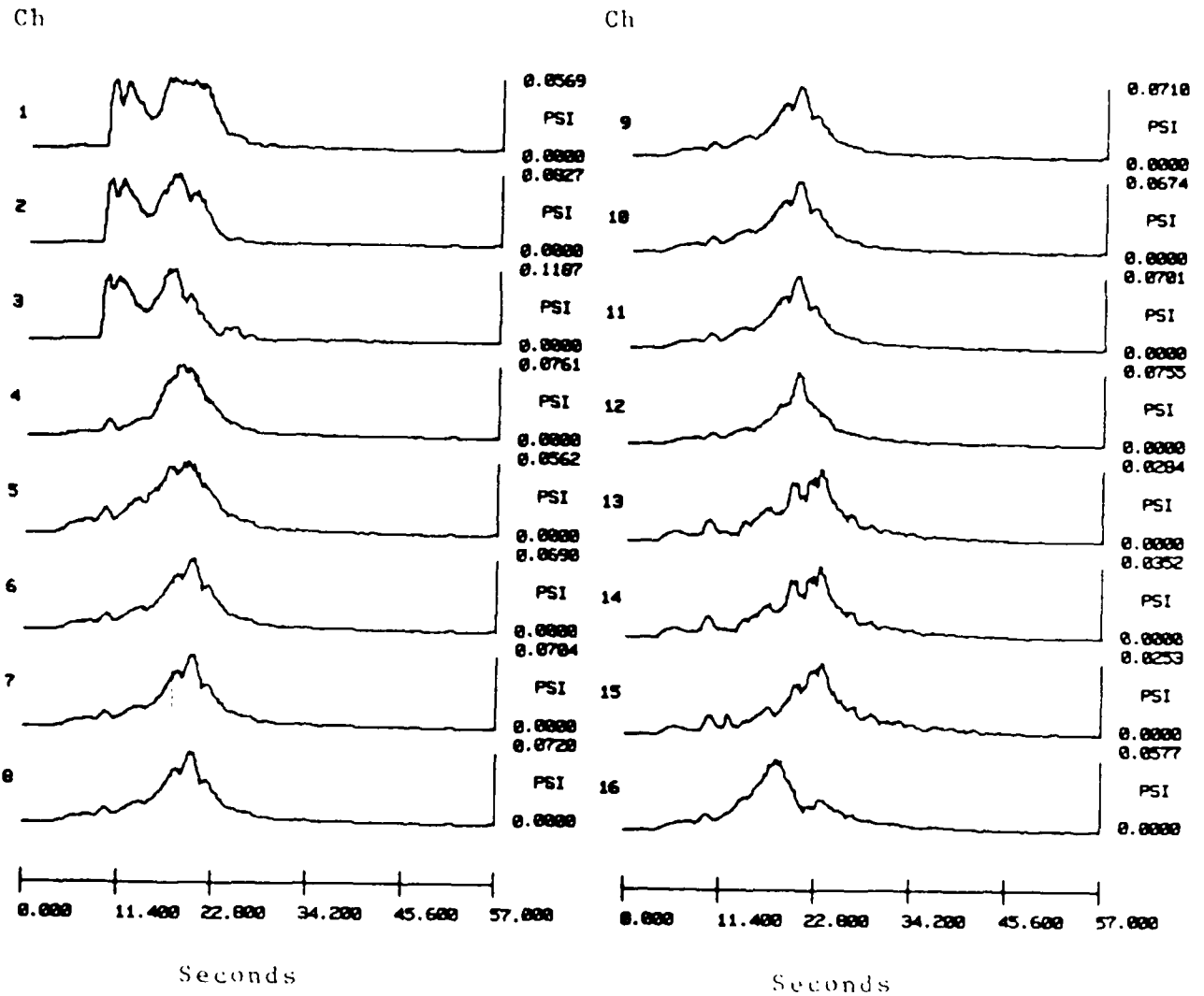
PHASE VELOCITY FOR IGNITION WAVELET
CHANNELS 6,7,8,10,11

FIGURE 8



PRESSURE EXTRAPOLATION AT EARLY LAUNCH TIMES

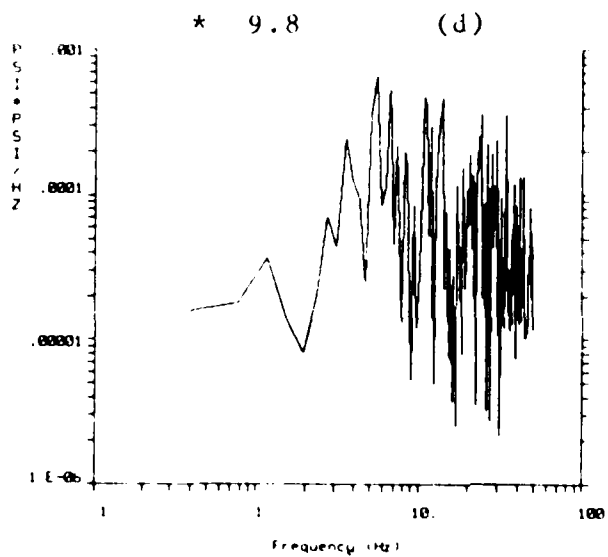
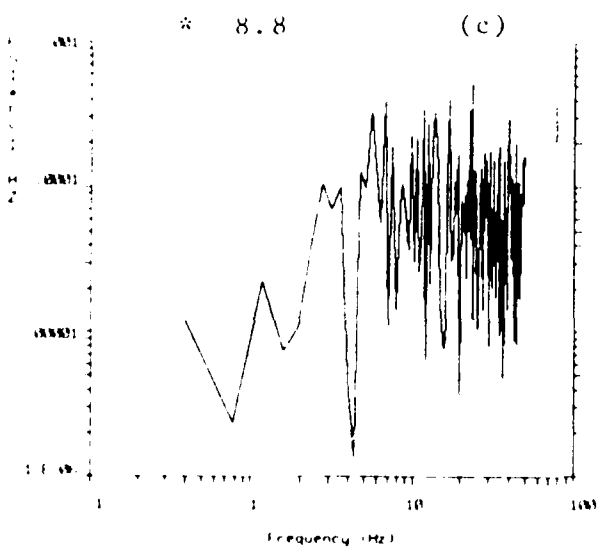
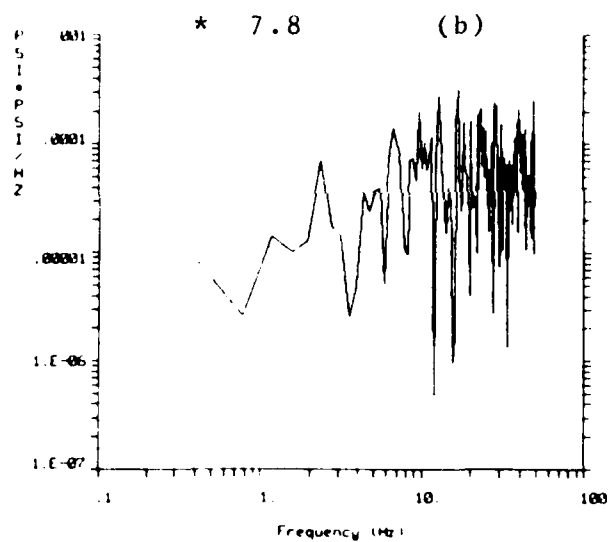
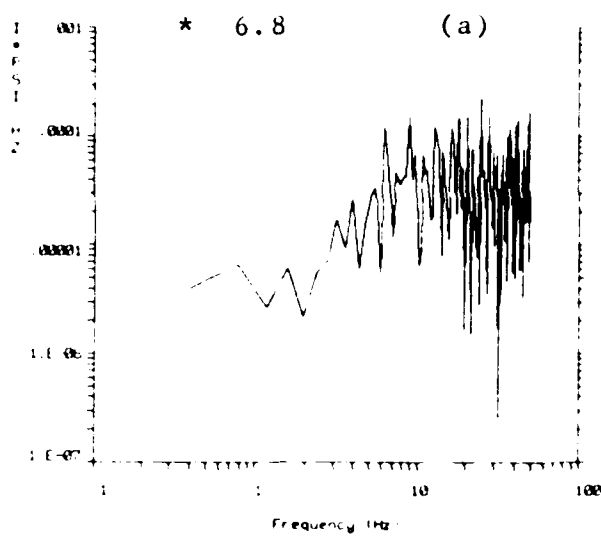
FIGURE 9



PLUME PRESSURE ENVELOPE

SPL (0,1.0)

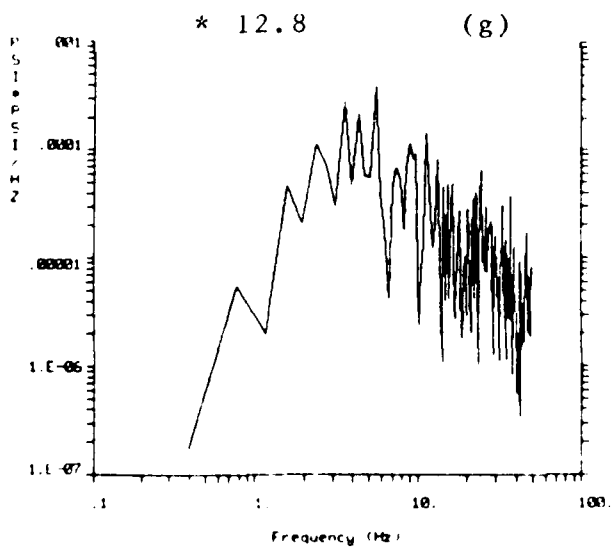
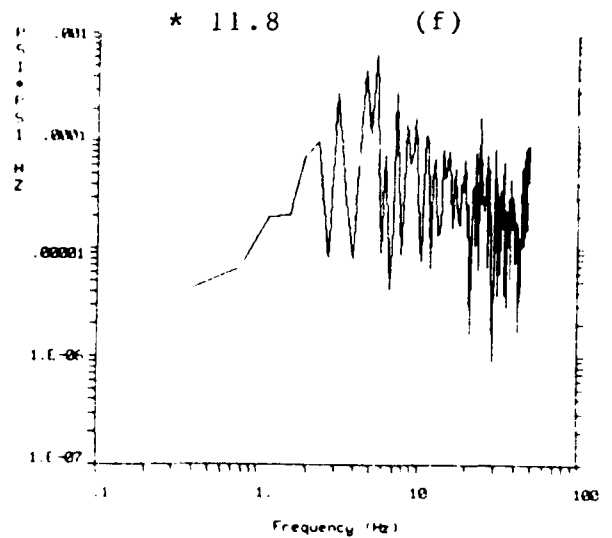
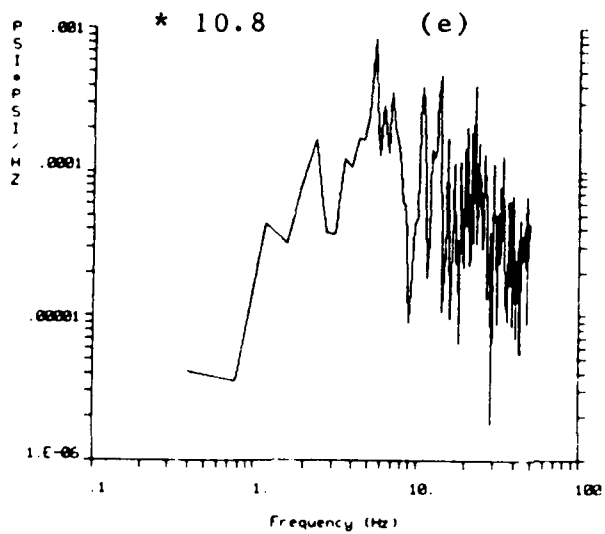
FIGURE 16



SURFACE PRESSURE SPECTRA

* Start Time
 DOF=12 <2.56> sec
 $R_0 \approx 300$ meters

FIGURES 11a thru 11d

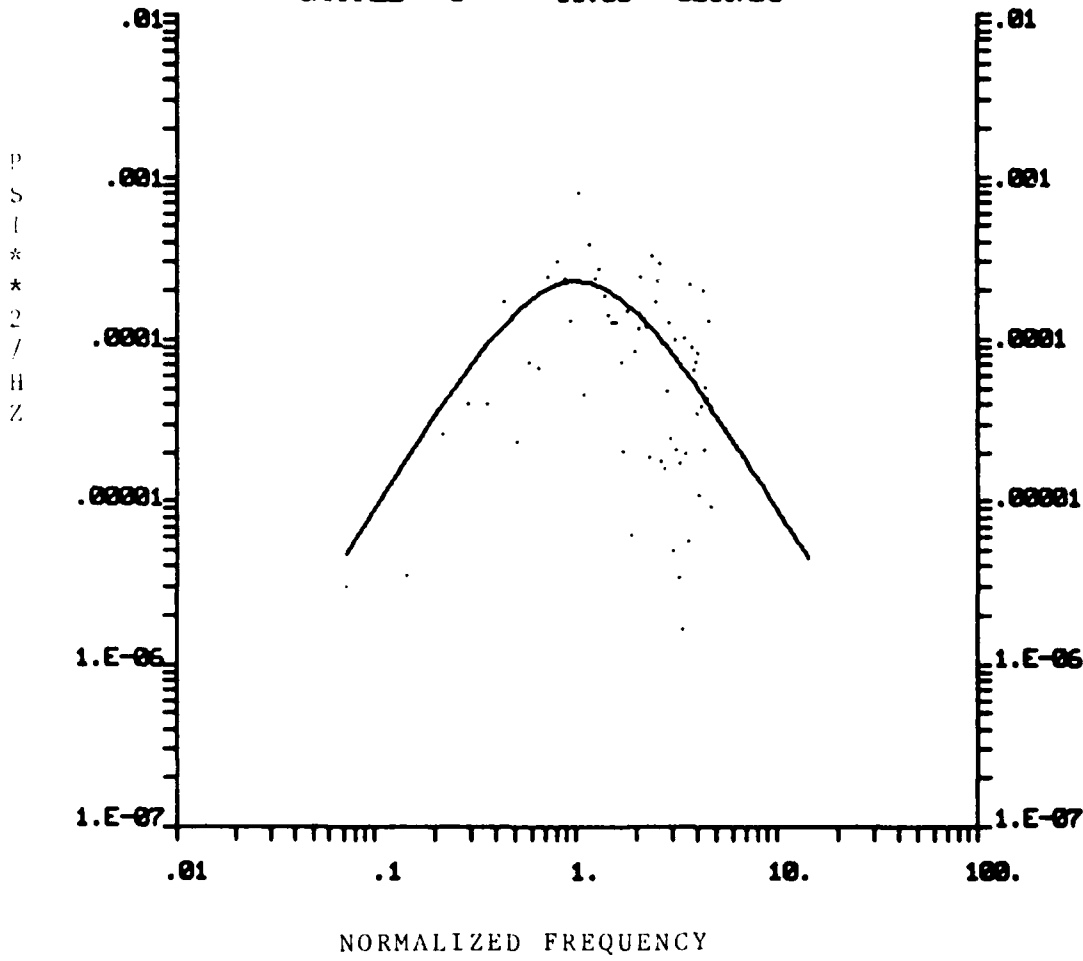


SURFACE PRESSURE SPECTRA

* Start Time
DOF=12 < 2.56 > sec
 $R_0 \approx 300$ meters

FIGURES 11e thru 11g

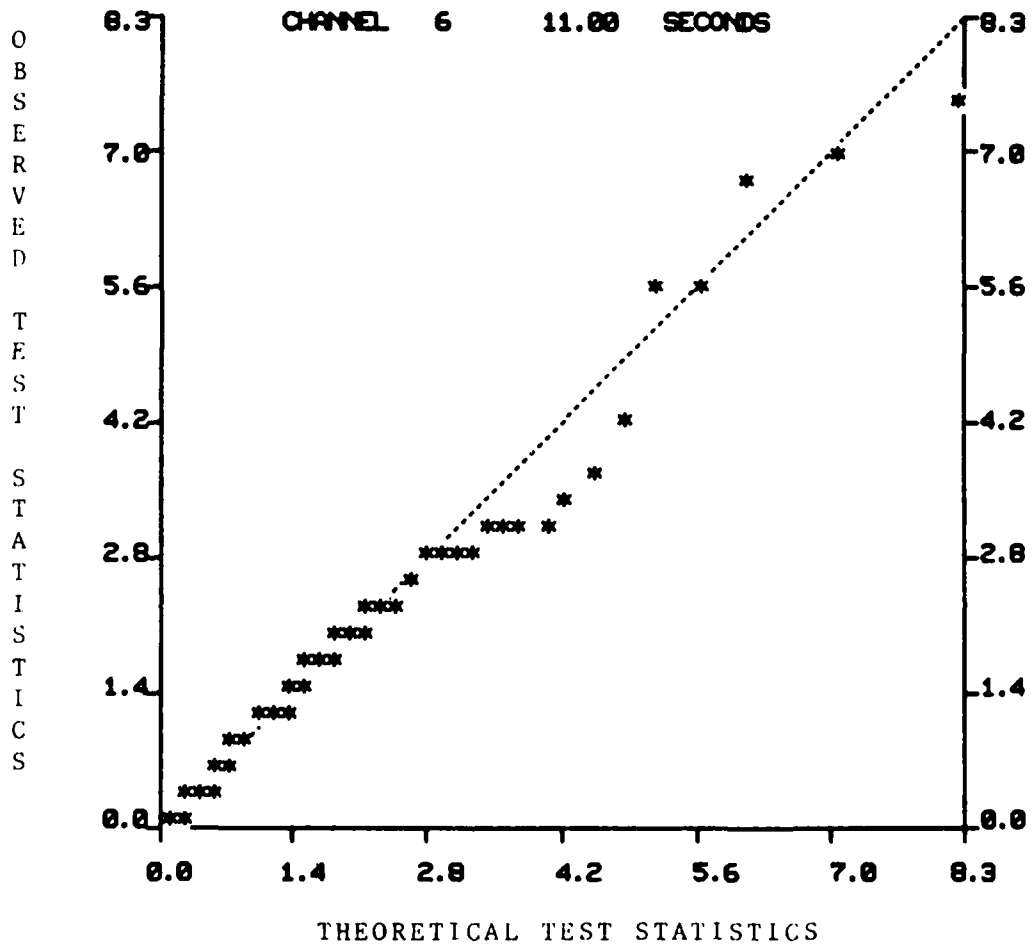
CHANNEL 6 11.00 SECONDS



OASPL = 3.88×10^{-3}
 $f_m = 5.4$ Hz
M = 0.9

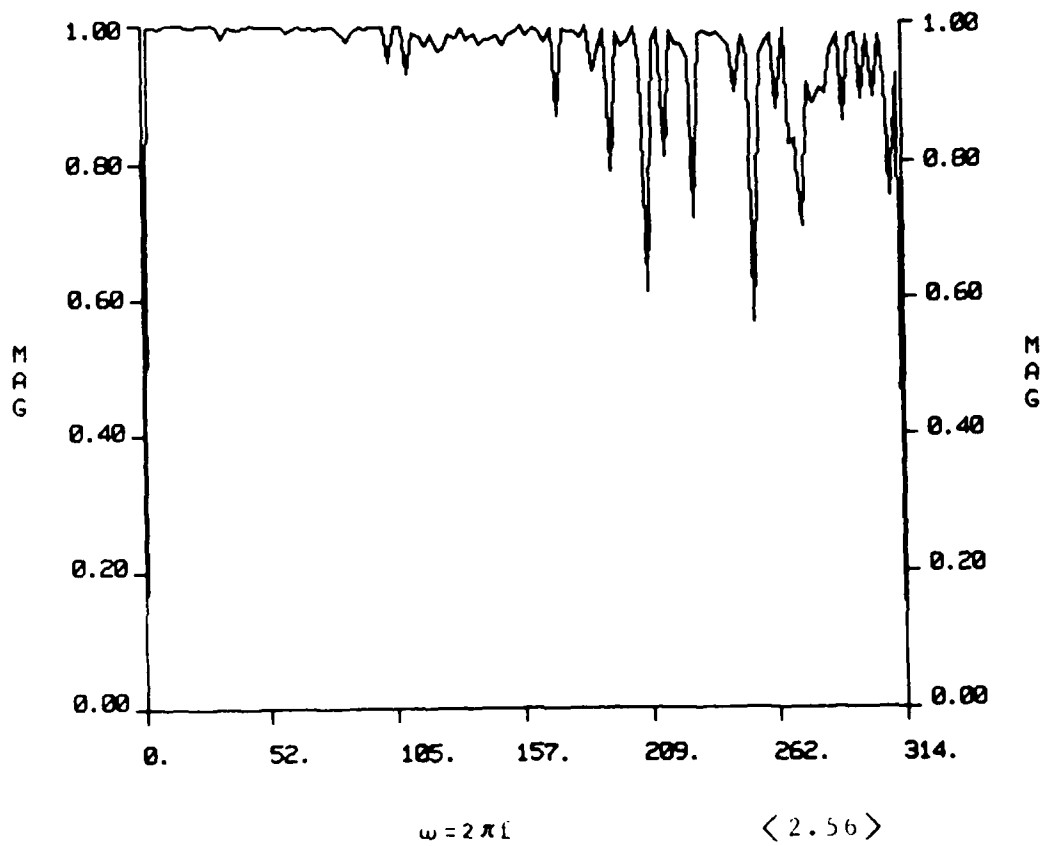
STANDARD FORM SPECTRA

FIGURE 12



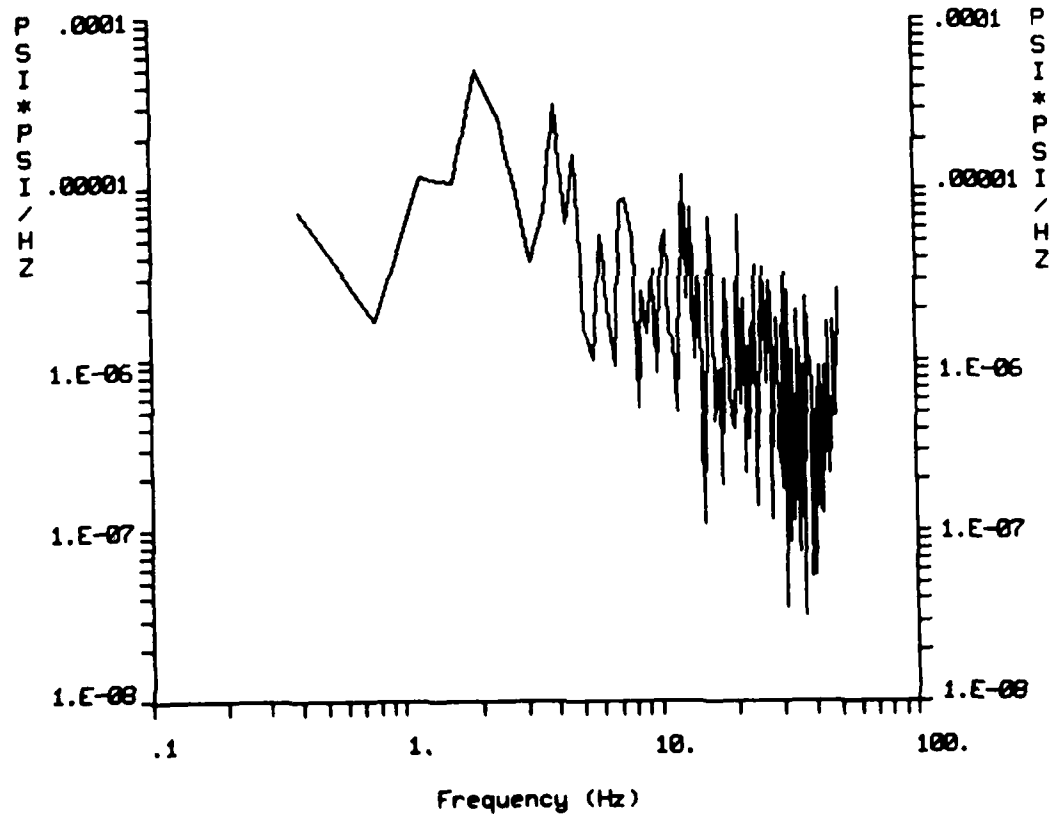
ACCEPTANCE TEST

FIGURE 13



$v(k, \omega)$ ABSOLUTE MAXIMA

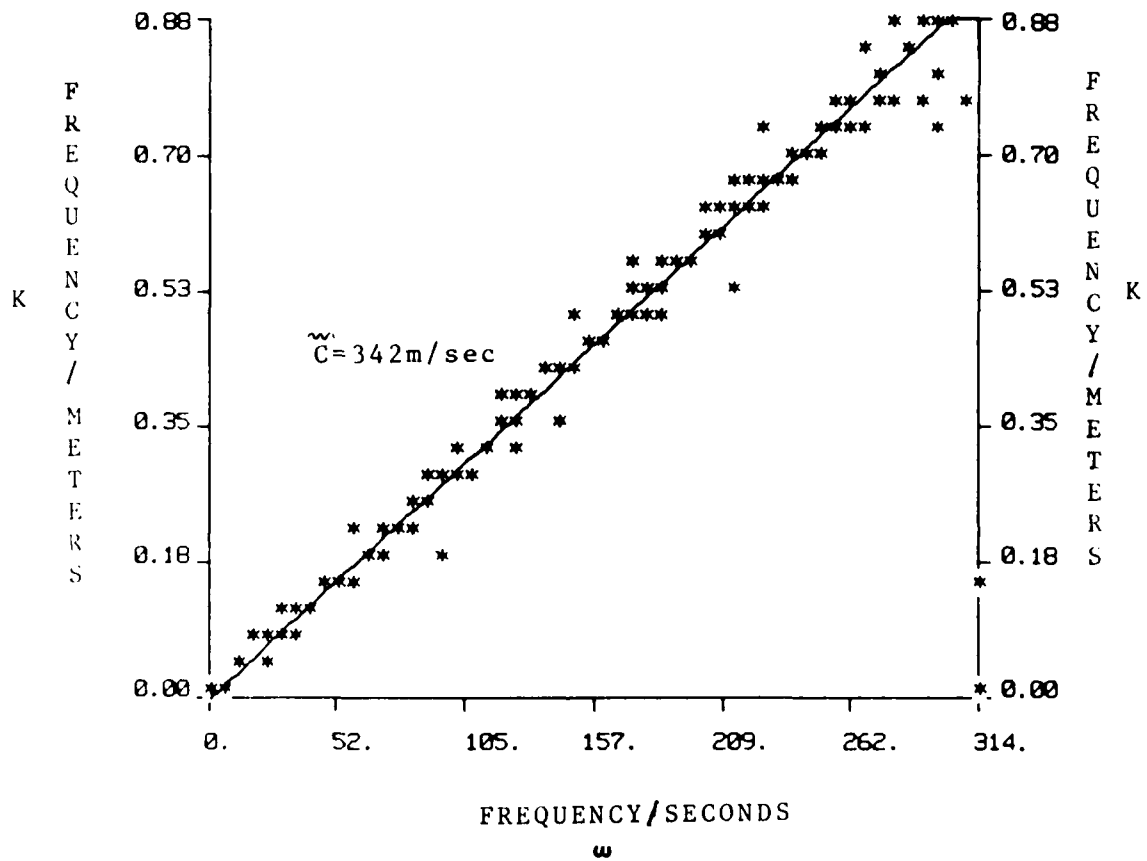
FIGURE 14



DOF 12 <2.56>

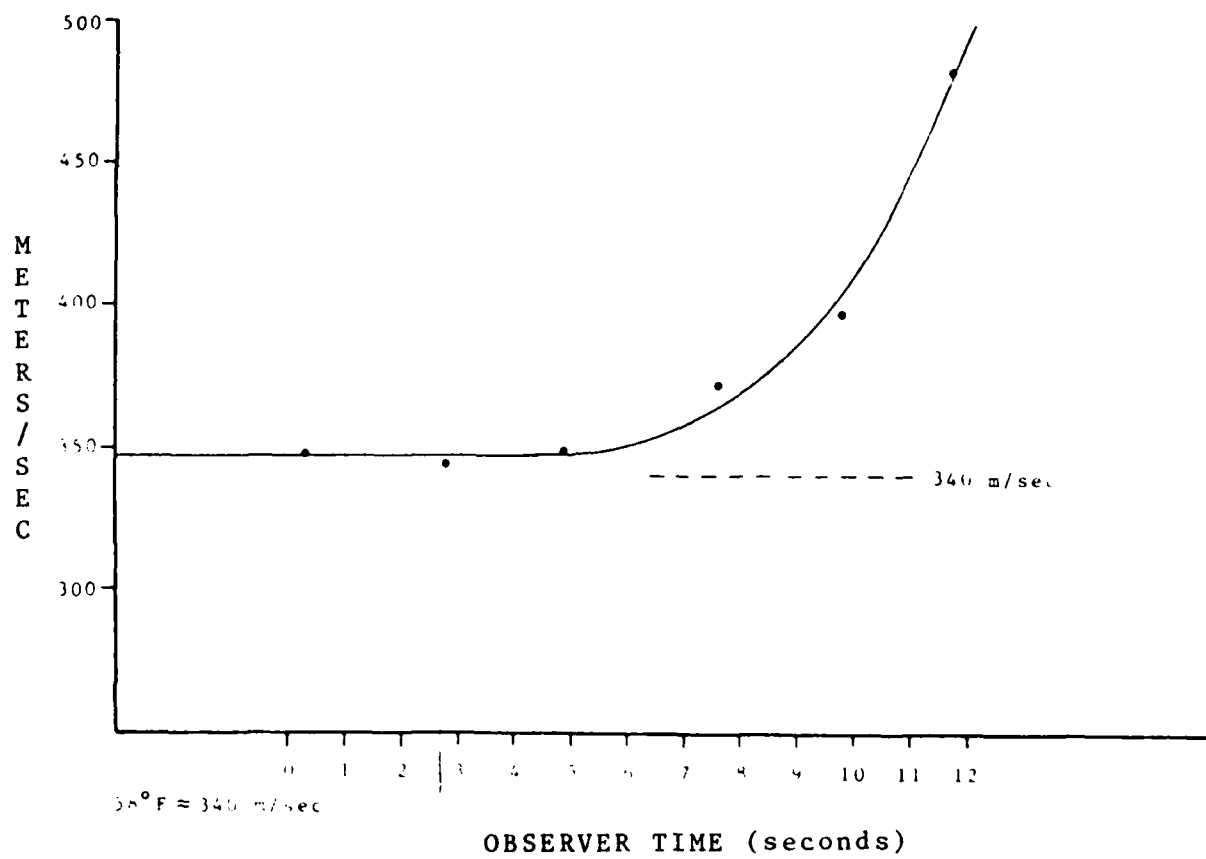
IGNITION WAVELET SPECTRA

FIGURE 15



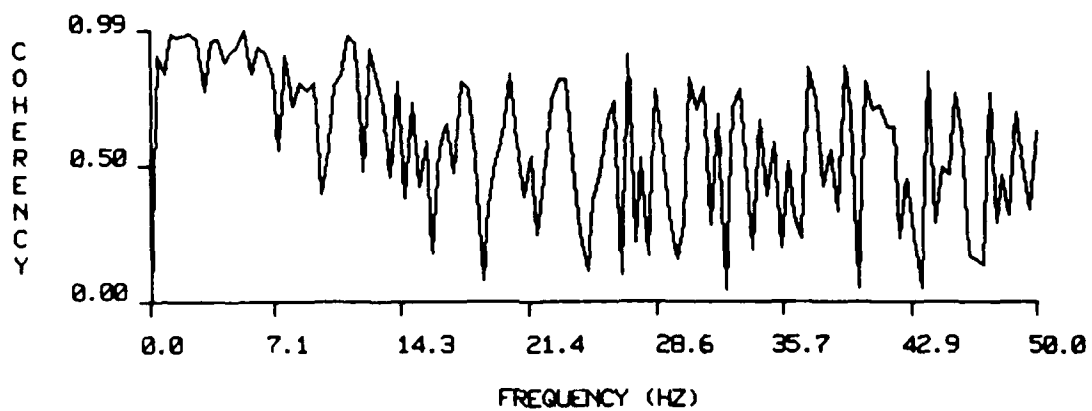
MEASURED PROPAGATION CHARACTERISTICS

FIGURE 16



MEDIAN PHASE VELOCITIES, METERS/SEC

FIGURE 17

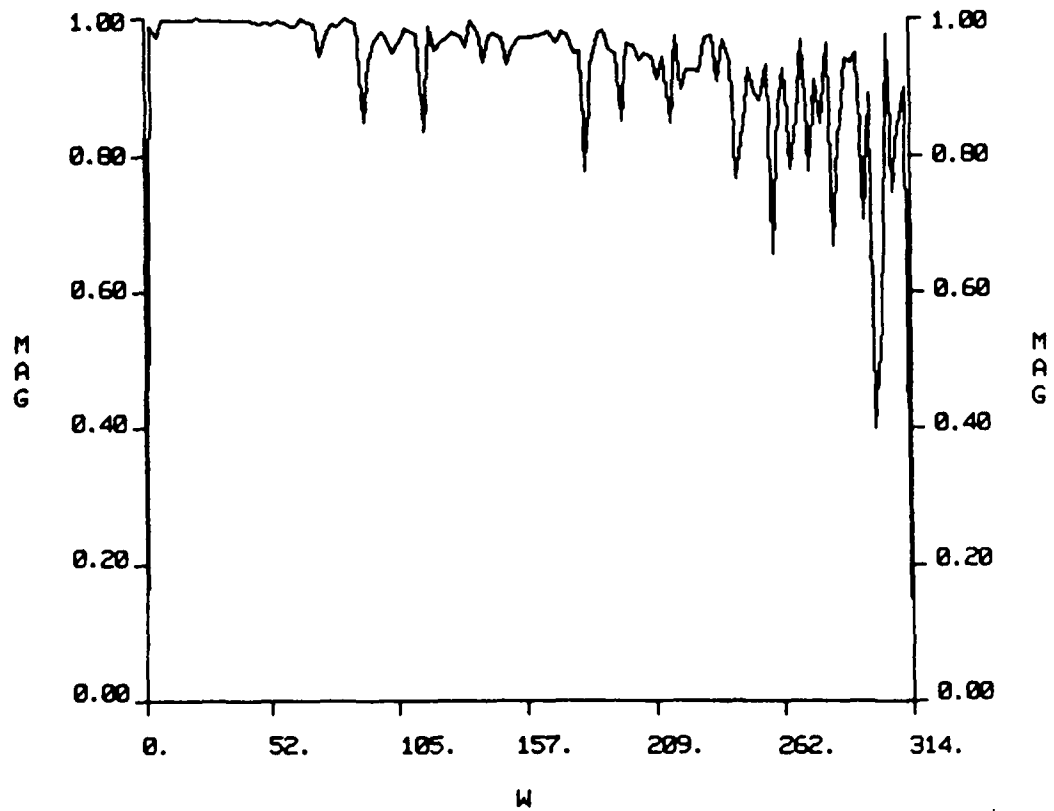


(6,12)

ORDINARY COHERENCY

$08:00:00.5 \leq t \leq 08:00:14.6$

FIGURE 18

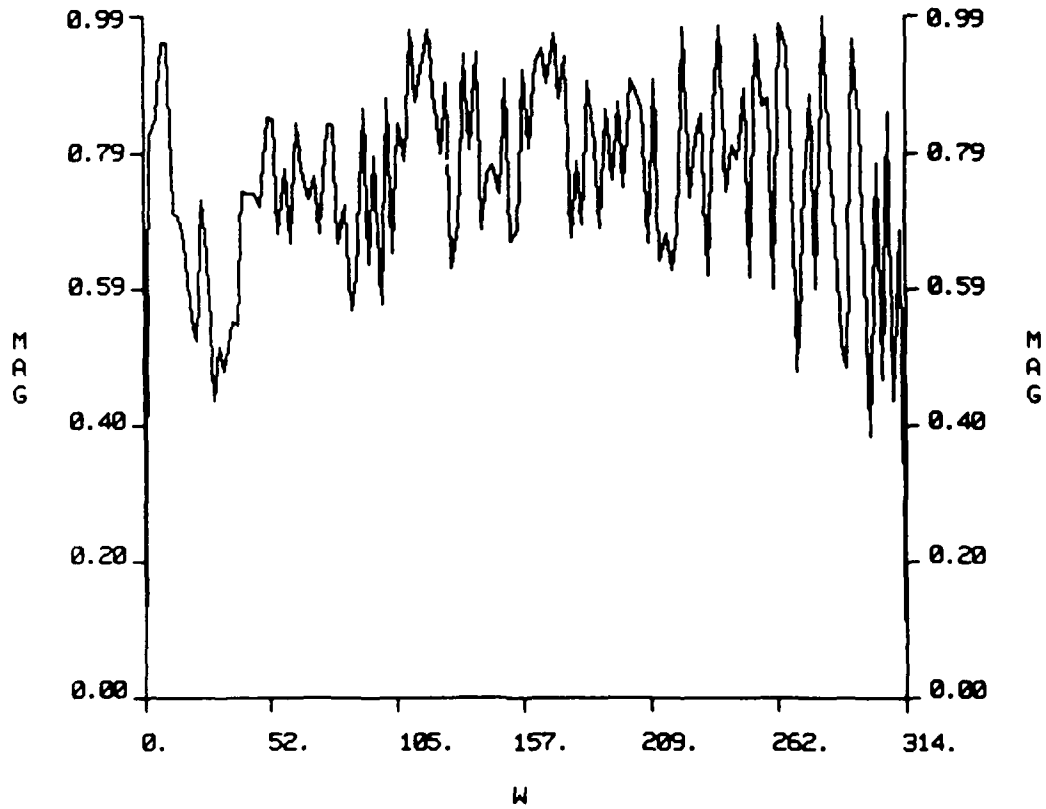


STATIONS 6,7,8,10,11

T=10.8

SPATIAL COHERENCY : 10 METERS

FIGURE 19

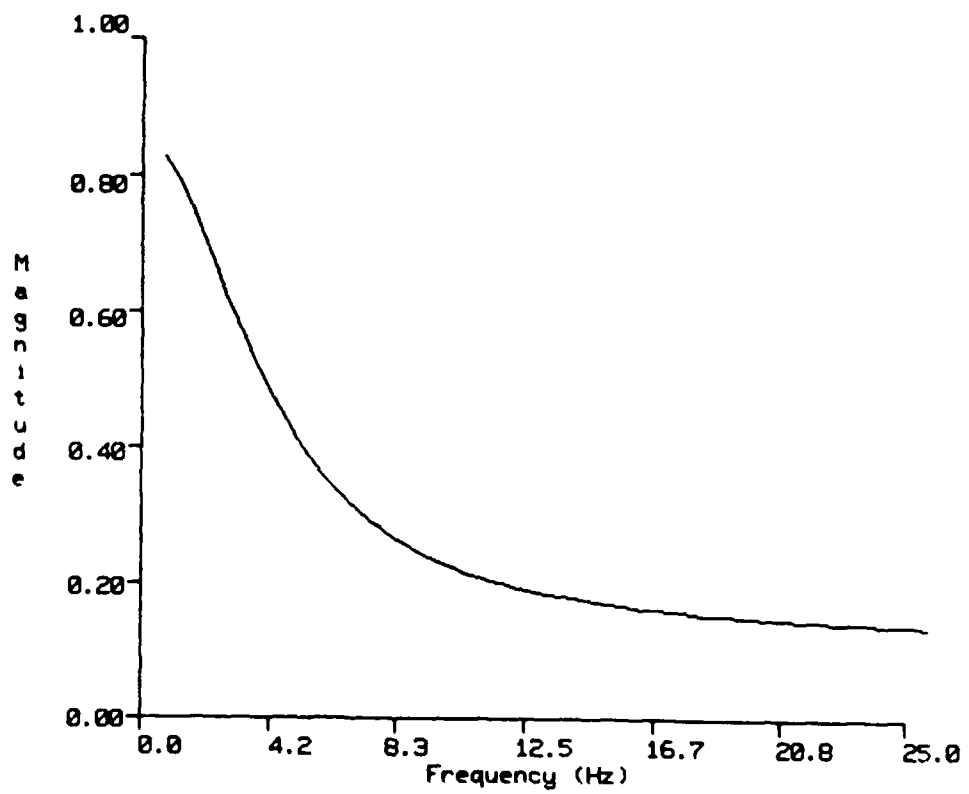


STATIONS 4,5,8,11,14

T=10.8

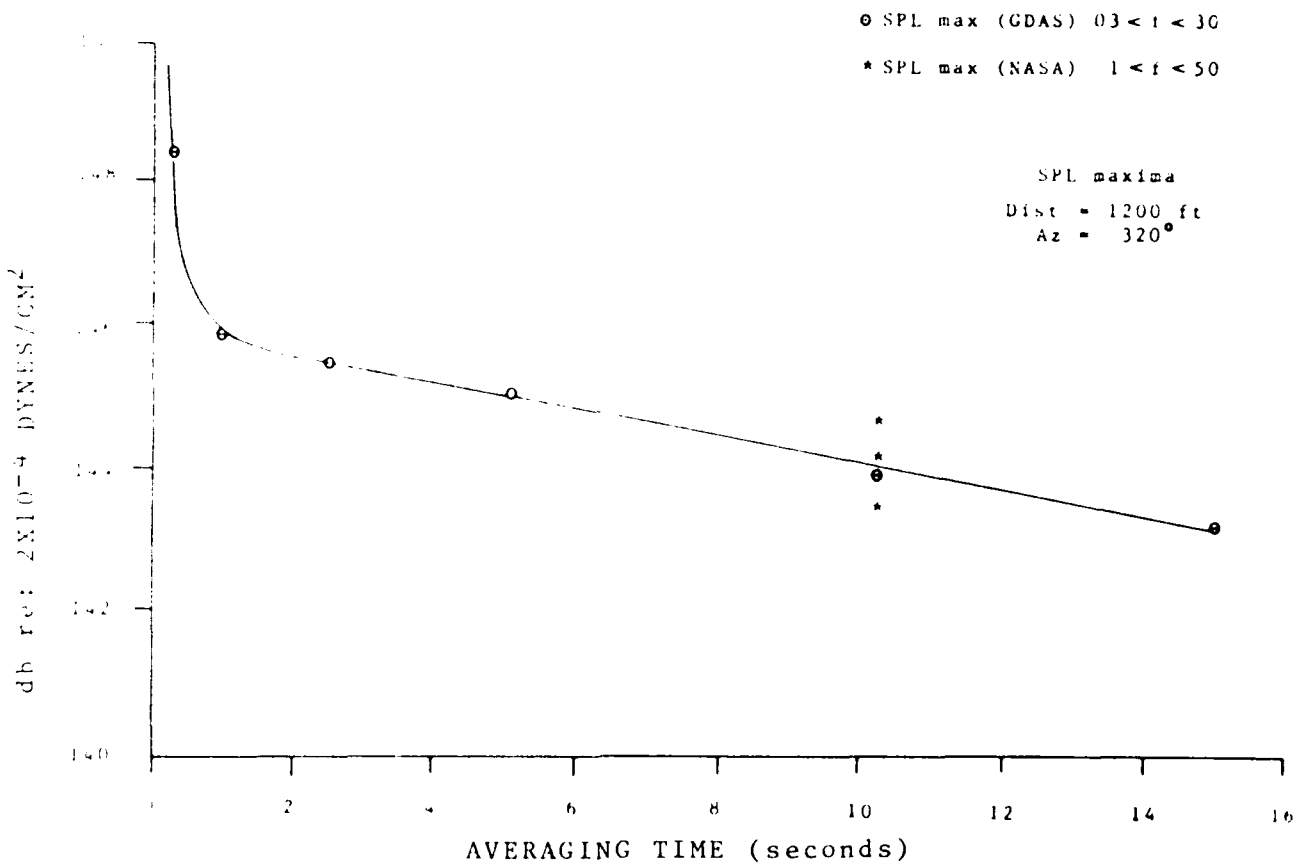
SPATIAL COHERENCY: 100 METERS

FIGURE 20



WATERCLOUD ATTENUATION ESTIMATE

FIGURE 21



SPL MAXIMA

FIGURE 22

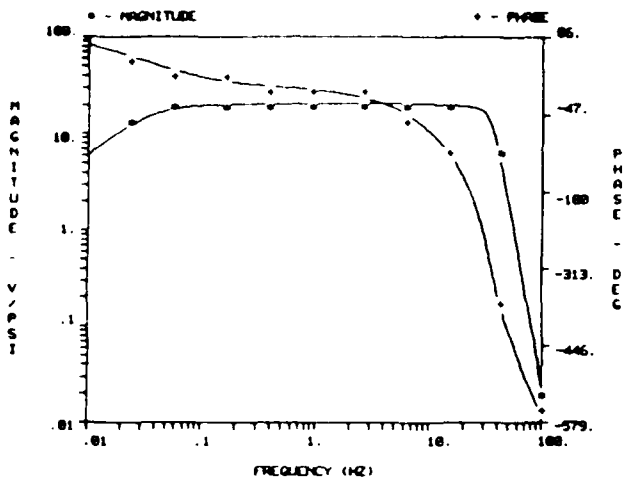
9.1 APPENDIX A, CHANNEL RESPONSES

CHANNEL 1

SENSOR:
 DC SCALE FACTOR - 4.510 (VOLTS/PSI)
 DC PHASE (DEGREES) - 100.0
 POLE FREQ (HZ) - 2000.

PREAMPLIFIER:
 DC GAIN (DB) - -64.33 DC PHASE (DEG) - 0.0000
 ZERO FREQ (HZ) - 0.1000E-04
 POLE FREQ (HZ) - 0.3240E-01
 POLE FREQ (HZ) - 100.0 DAMP COEFF - 0.7070

FILTER:
 STAGE 1
 DC GAIN (DB) - 7.092 DC PHASE (DEG) - 0.0000
 POLE FREQ (HZ) - 670.0
 STAGE 2
 DC GAIN (DB) - 0.1217 DC PHASE (DEG) - 100.0
 POLE FREQ (HZ) - 34.19 DAMP COEFF - 1.000
 STAGE 3
 DC GAIN (DB) - 0.3730E-02 DC PHASE (DEG) - 0.0000
 POLE FREQ (HZ) - 34.34 DAMP COEFF - 0.7200
 STAGE 4
 DC GAIN (DB) - -0.8670E-02 DC PHASE (DEG) - 100.0
 POLE FREQ (HZ) - 1591.
 STAGE 5
 DC GAIN (DB) - 0.6423E-01 DC PHASE (DEG) - 100.0
 POLE FREQ (HZ) - 34.16 DAMP COEFF - 0.2600

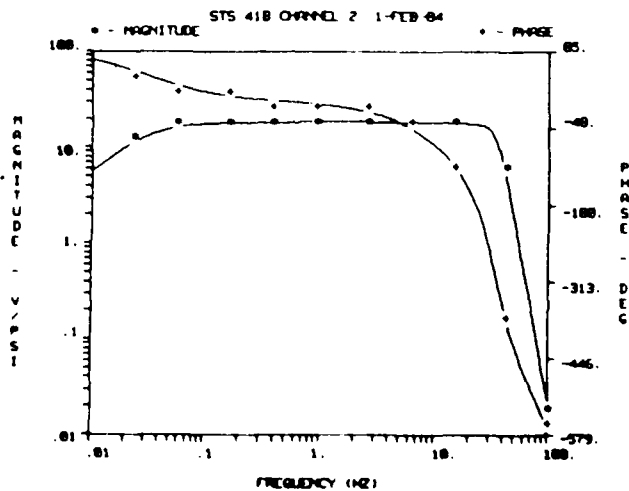


CHANNEL 2

SENSOR:
 DC SCALE FACTOR - 3.790 (VOLTS/PSI)
 DC PHASE (DEGREES) - 100.0
 POLE FREQ (HZ) - 2000.

PREAMPLIFIER:
 DC GAIN (DB) - -64.00 DC PHASE (DEG) - 0.0000
 ZERO FREQ (HZ) - 0.1000E-04
 POLE FREQ (HZ) - 0.3120E-01
 POLE FREQ (HZ) - 100.0 DAMP COEFF - 0.7070

FILTER:
 STAGE 1
 DC GAIN (DB) - 7.915 DC PHASE (DEG) - 0.0000
 POLE FREQ (HZ) - 670.0
 STAGE 2
 DC GAIN (DB) - 0.3625E-01 DC PHASE (DEG) - 100.0
 POLE FREQ (HZ) - 34.17 DAMP COEFF - 1.000
 STAGE 3
 DC GAIN (DB) - -0.2057E-01 DC PHASE (DEG) - 0.0000
 POLE FREQ (HZ) - 34.34 DAMP COEFF - 0.7200
 STAGE 4
 DC GAIN (DB) - -0.5210E-02 DC PHASE (DEG) - 100.0
 POLE FREQ (HZ) - 1592.
 STAGE 5
 DC GAIN (DB) - -0.2167E-01 DC PHASE (DEG) - 100.0
 POLE FREQ (HZ) - 34.32 DAMP COEFF - 0.2600



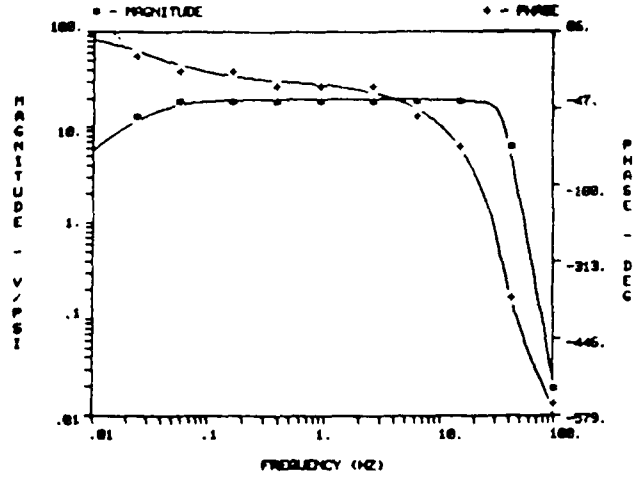
CHANNEL RESPONSES

CHANNEL 3

SENSOR:
 DC SCALE FACTOR - 4.418 (VOLTS/PSI)
 DC PHASE (DEGREES) - 180.0
 POLE FREQ (HZ) - 2000.

PREAMPLIFIER:
 DC GAIN (DB) - -64.49 DC PHASE (DEG) - 0.0000
 ZERO FREQ (HZ) - 0.1800E-04
 POLE FREQ (HZ) - 0.3300E-01 DAMP COEFF - 0.7070
 POLE FREQ (HZ) - 100.0

FILTER:
 STAGE 1
 DC GAIN (DB) - 7.092 DC PHASE (DEG) - 0.0000
 POLE FREQ (HZ) - 678.0
 STAGE 2
 DC GAIN (DB) - 0.1065E-01 DC PHASE (DEG) - 180.0
 POLE FREQ (HZ) - 34.25 DAMP COEFF - 1.005
 STAGE 3
 DC GAIN (DB) - 0.3359E-01 DC PHASE (DEG) - 0.0000
 POLE FREQ (HZ) - 34.25 DAMP COEFF - 0.7327
 STAGE 4
 DC GAIN (DB) - -0.8687E-03 DC PHASE (DEG) - 180.0
 POLE FREQ (HZ) - 1592.
 STAGE 5
 DC GAIN (DB) - 0.1298E-01 DC PHASE (DEG) - 180.0
 POLE FREQ (HZ) - 34.33 DAMP COEFF - 0.2609

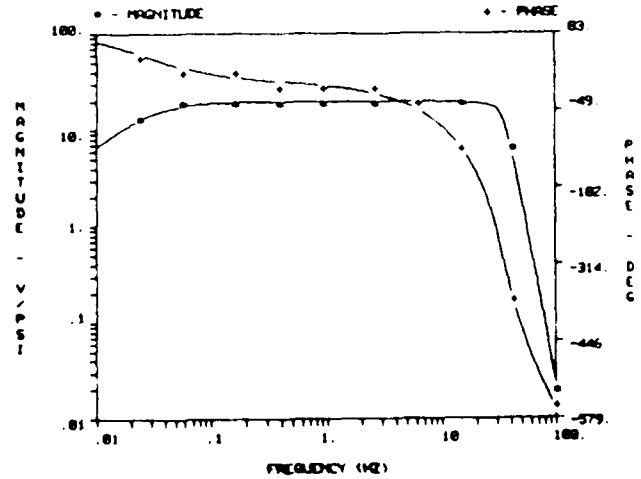


CHANNEL 4

SENSOR:
 DC SCALE FACTOR - 3.298 (VOLTS/PSI)
 DC PHASE (DEGREES) - 180.0
 POLE FREQ (HZ) - 2000.

PREAMPLIFIER:
 DC GAIN (DB) - -63.01 DC PHASE (DEG) - 0.0000
 ZERO FREQ (HZ) - 0.1800E-04
 POLE FREQ (HZ) - 0.2798E-01 DAMP COEFF - 0.7070
 POLE FREQ (HZ) - 100.0

FILTER:
 STAGE 1
 DC GAIN (DB) - 9.600 DC PHASE (DEG) - 0.0000
 POLE FREQ (HZ) - 678.0
 STAGE 2
 DC GAIN (DB) - 0.1546E-01 DC PHASE (DEG) - 180.0
 POLE FREQ (HZ) - 34.35 DAMP COEFF - 0.9903
 STAGE 3
 DC GAIN (DB) - 0.1124E-01 DC PHASE (DEG) - 0.0000
 POLE FREQ (HZ) - 34.33 DAMP COEFF - 0.7325
 STAGE 4
 DC GAIN (DB) - -0.7800E-02 DC PHASE (DEG) - 180.0
 POLE FREQ (HZ) - 1589.
 STAGE 5
 DC GAIN (DB) - 0.5700E-01 DC PHASE (DEG) - 180.0
 POLE FREQ (HZ) - 34.33 DAMP COEFF - 0.2679



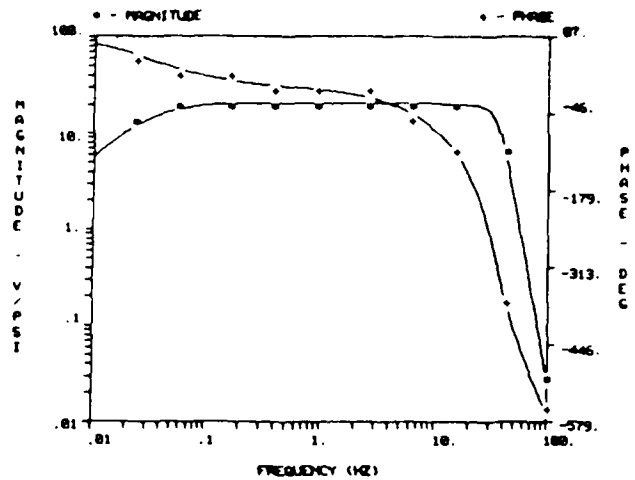
CHANNEL RESPONSES

CHANNEL 5

SENSOR:
 DC SCALE FACTOR - 4.188 (VOLTS/PSI)
 DC PHASE (DEGREES) - 180.0
 POLE FREQ (HZ) - 2888.

PREAMPLIFIER:
 DC GAIN (DB) - -64.76 DC PHASE (DEG) - 0.0000
 ZERO FREQ (HZ) - 0.1800E-04
 POLE FREQ (HZ) - 0.3418E-01 DAMP COEFF - 0.7878
 POLE FREQ (HZ) - 188.0

FILTER:
 STAGE 1
 DC GAIN (DB) - 7.915 DC PHASE (DEG) - 0.0000
 POLE FREQ (HZ) - 678.0
 STAGE 2
 DC GAIN (DB) - -0.3960E-01 DC PHASE (DEG) - 180.0
 POLE FREQ (HZ) - 34.29 DAMP COEFF - 1.082
 STAGE 3
 DC GAIN (DB) - -0.4120E-01 DC PHASE (DEG) - 0.0000
 POLE FREQ (HZ) - 34.46 DAMP COEFF - 0.7281
 STAGE 4
 DC GAIN (DB) - -0.1216E-01 DC PHASE (DEG) - 180.0
 POLE FREQ (HZ) - 1592.
 STAGE 5
 DC GAIN (DB) - 0.5638E-01 DC PHASE (DEG) - 180.0
 POLE FREQ (HZ) - 34.23 DAMP COEFF - 0.2688

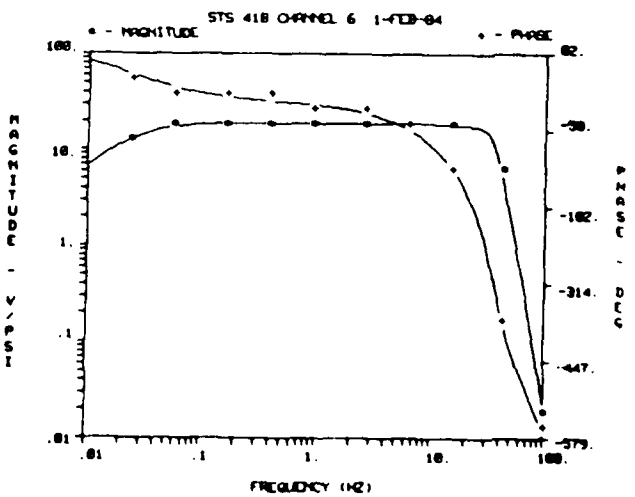


CHANNEL 6

SENSOR:
 DC SCALE FACTOR - 2.988 (VOLTS/PSI)
 DC PHASE (DEGREES) - 180.0
 POLE FREQ (HZ) - 2800.

PREAMPLIFIER:
 DC GAIN (DB) - -62.58 DC PHASE (DEG) - 0.0000
 ZERO FREQ (HZ) - 0.1800E-04
 POLE FREQ (HZ) - 0.2658E-01 DAMP COEFF - 0.7878
 POLE FREQ (HZ) - 188.0

FILTER:
 STAGE 1
 DC GAIN (DB) - 18.43 DC PHASE (DEG) - 0.0000
 POLE FREQ (HZ) - 678.0
 STAGE 2
 DC GAIN (DB) - -0.1287 DC PHASE (DEG) - 180.0
 POLE FREQ (HZ) - 34.26 DAMP COEFF - 1.084
 STAGE 3
 DC GAIN (DB) - 0.9717E-01 DC PHASE (DEG) - 0.0000
 POLE FREQ (HZ) - 34.19 DAMP COEFF - 0.7345
 STAGE 4
 DC GAIN (DB) - -0.1735E-01 DC PHASE (DEG) - 180.0
 POLE FREQ (HZ) - 1591.
 STAGE 5
 DC GAIN (DB) - 0.1541E-01 DC PHASE (DEG) - 180.0
 POLE FREQ (HZ) - 34.26 DAMP COEFF - 0.2781



CHANNEL RESPONSES

CHANNEL 7

SENSOR:

DC SCALE FACTOR * 2.938 (VOLTS/PSI)
 DC PHASE (DEGREES) * 188.8
 POLE FREQ (HZ) * 2000.

PREAMPLIFIER:

DC GAIN (DB) * -64.17 DC PHASE (DEG) * 0.0000
 ZERO FREQ (HZ) * 0.1000E-04
 POLE FREQ (HZ) * 0.3100E-01 DAMP COEFF * 0.7070
 POLE FREQ (HZ) * 100.0

FILTER:

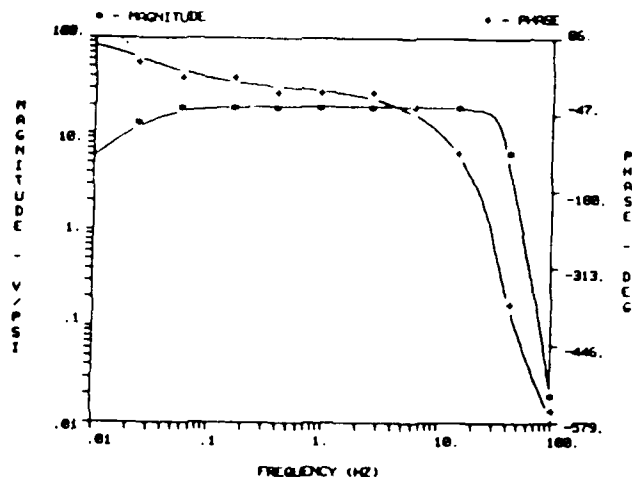
STAGE 1
 DC GAIN (DB) * 18.43 DC PHASE (DEG) * 0.0000
 POLE FREQ (HZ) * 670.0

STAGE 2
 DC GAIN (DB) * -0.2010E-01 DC PHASE (DEG) * 188.0
 POLE FREQ (HZ) * 34.23 DAMP COEFF * 1.006

STAGE 3
 DC GAIN (DB) * 0.1875E-02 DC PHASE (DEG) * 0.0000
 POLE FREQ (HZ) * 34.28 DAMP COEFF * 0.7363

STAGE 4
 DC GAIN (DB) * -0.8681E-02 DC PHASE (DEG) * 188.0
 POLE FREQ (HZ) * 1592.

STAGE 5
 DC GAIN (DB) * 0.5370E-01 DC PHASE (DEG) * 188.0
 POLE FREQ (HZ) * 34.14 DAMP COEFF * 0.2681



CHANNEL 8

SENSOR:

DC SCALE FACTOR * 3.998 (VOLTS/PSI)
 DC PHASE (DEGREES) * 188.8
 POLE FREQ (HZ) * 2000.

PREAMPLIFIER:

DC GAIN (DB) * -63.84 DC PHASE (DEG) * 0.0000
 ZERO FREQ (HZ) * 0.1000E-04
 POLE FREQ (HZ) * 0.3070E-01 DAMP COEFF * 0.7070
 POLE FREQ (HZ) * 100.0

FILTER:

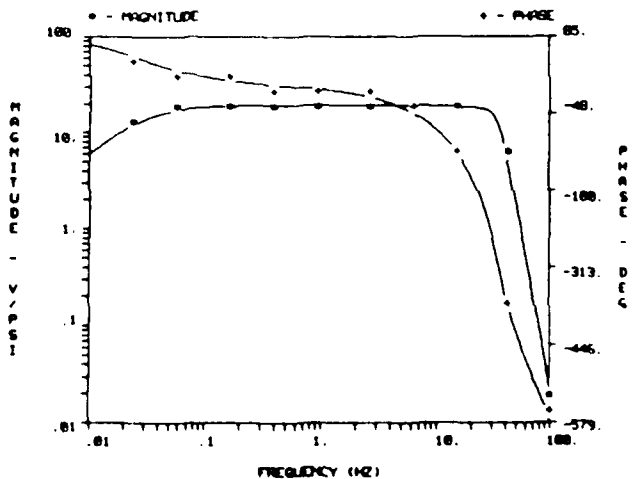
STAGE 1
 DC GAIN (DB) * 8.743 DC PHASE (DEG) * 0.0000
 POLE FREQ (HZ) * 670.0

STAGE 2
 DC GAIN (DB) * -0.3142E-01 DC PHASE (DEG) * 188.0
 POLE FREQ (HZ) * 34.39 DAMP COEFF * 1.001

STAGE 3
 DC GAIN (DB) * -0.1691E-01 DC PHASE (DEG) * 0.0000
 POLE FREQ (HZ) * 34.43 DAMP COEFF * 0.7387

STAGE 4
 DC GAIN (DB) * -0.1129E-01 DC PHASE (DEG) * 188.0
 POLE FREQ (HZ) * 1592.

STAGE 5
 DC GAIN (DB) * 0.1737E-02 DC PHASE (DEG) * 188.0
 POLE FREQ (HZ) * 34.43 DAMP COEFF * 0.2681



CHANNEL RESPONSES

CHANNEL 9

SENSOR:

DC GAIN FACTOR - 3.578 (VOLTS/PSI)
 DC PHASE (DEGREES) - 180.0
 POLE FREQ (HZ) - 2800.

PREAMPLIFIER:

DC GAIN (DB) - -64.58 DC PHASE (DEG) - 0.0000
 ZERO FREQ (HZ) - 0.1000E-04
 POLE FREQ (HZ) - 0.3316E-01 DAMP COEFF - 0.7878
 POLE FREQ (HZ) - 188.0

FILTER:

STAGE 1

DC GAIN (DB) - 9.680 DC PHASE (DEG) - 0.0000
 POLE FREQ (HZ) - 678.0

STAGE 2

DC GAIN (DB) - -0.3298E-01 DC PHASE (DEG) - 180.0
 POLE FREQ (HZ) - 34.34 DAMP COEFF - 1.002

STAGE 3

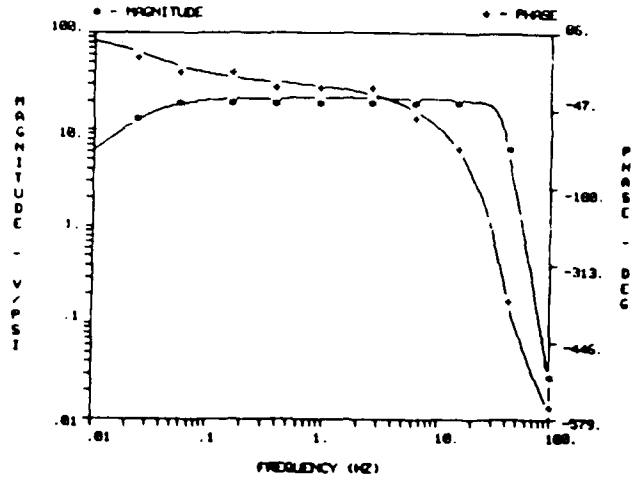
DC GAIN (DB) - -0.7479E-02 DC PHASE (DEG) - 0.0000
 POLE FREQ (HZ) - 34.31 DAMP COEFF - 0.7333

STAGE 4

DC GAIN (DB) - 0.2601E-02 DC PHASE (DEG) - 180.0
 POLE FREQ (HZ) - 1589.

STAGE 5

DC GAIN (DB) - -0.1381E-01 DC PHASE (DEG) - 180.0
 POLE FREQ (HZ) - 34.39 DAMP COEFF - 0.2635



CHANNEL 10

SENSOR:

DC GAIN FACTOR - 3.228 (VOLTS/PSI)
 DC PHASE (DEGREES) - 180.0
 POLE FREQ (HZ) - 2800.

PREAMPLIFIER:

DC GAIN (DB) - -63.88 DC PHASE (DEG) - 0.0000
 ZERO FREQ (HZ) - 0.1000E-04
 POLE FREQ (HZ) - 0.2816E-01 DAMP COEFF - 0.7878
 POLE FREQ (HZ) - 188.0

FILTER:

STAGE 1

DC GAIN (DB) - 9.680 DC PHASE (DEG) - 0.0000
 POLE FREQ (HZ) - 678.0

STAGE 2

DC GAIN (DB) - -0.4789E-01 DC PHASE (DEG) - 180.0
 POLE FREQ (HZ) - 34.37 DAMP COEFF - 1.002

STAGE 3

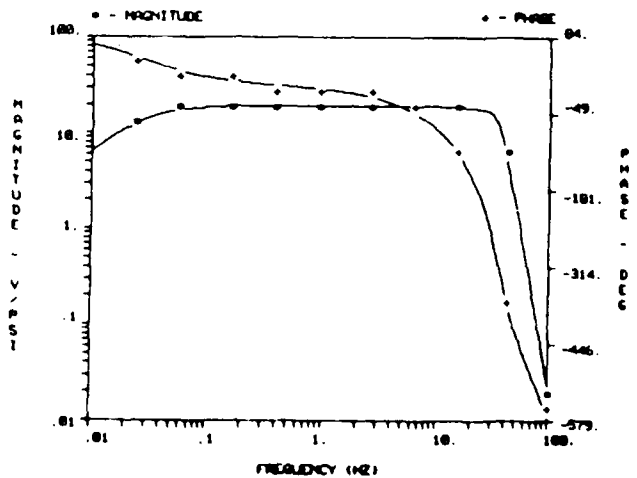
DC GAIN (DB) - 0.3177E-01 DC PHASE (DEG) - 0.0000
 POLE FREQ (HZ) - 34.26 DAMP COEFF - 0.7241

STAGE 4

DC GAIN (DB) - 0.1381E-01 DC PHASE (DEG) - 180.0
 POLE FREQ (HZ) - 1589.

STAGE 5

DC GAIN (DB) - 0.0848E-01 DC PHASE (DEG) - 180.0
 POLE FREQ (HZ) - 34.16 DAMP COEFF - 0.2635



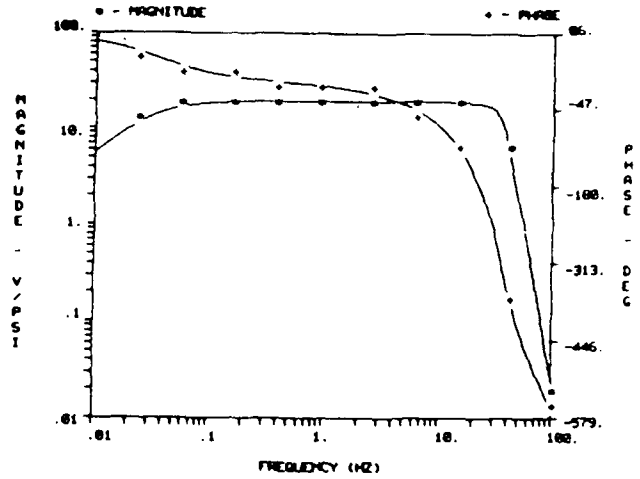
CHANNEL RESPONSES

CHANNEL 11

SENSOR:
 DC SCALE FACTOR - 4.468 (VOLTS/PSI)
 DC PHASE (DEGREES) - 180.0
 POLE FREQ (HZ) - 2880.

PREAMPLIFIER:
 DC GAIN (DB) - -64.53 DC PHASE (DEG) - 0.0000
 ZERO FREQ (HZ) - 0.1000E-04
 POLE FREQ (HZ) - 0.3320E-01
 POLE FREQ (HZ) - 100.0 DAMP COEFF - 0.7070

FILTER:
 STAGE 1
 DC GAIN (DB) - 7.087 DC PHASE (DEG) - 0.0000
 POLE FREQ (HZ) - 670.0
 STAGE 2
 DC GAIN (DB) - -0.6119E-01 DC PHASE (DEG) - 180.0
 POLE FREQ (HZ) - 34.42 DAMP COEFF - 1.000
 STAGE 3
 DC GAIN (DB) - -0.1127E-01 DC PHASE (DEG) - 0.0000
 POLE FREQ (HZ) - 34.31 DAMP COEFF - 0.7340
 STAGE 4
 DC GAIN (DB) - -0.1650E-01 DC PHASE (DEG) - 180.0
 POLE FREQ (HZ) - 1593.
 STAGE 5
 DC GAIN (DB) - -0.7756E-01 DC PHASE (DEG) - 180.0
 POLE FREQ (HZ) - 34.40 DAMP COEFF - 0.2670

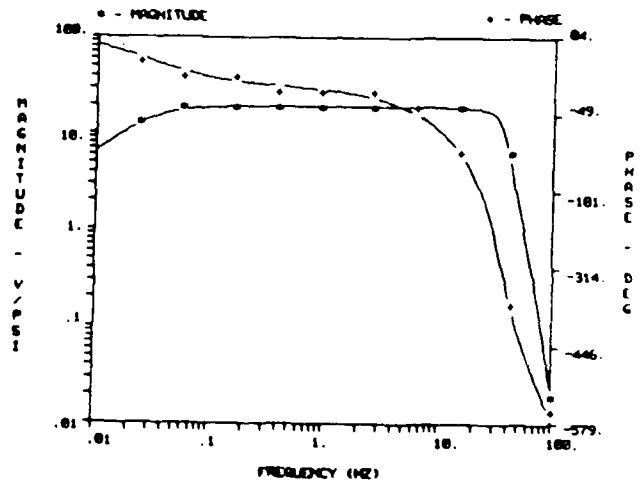


CHANNEL 12

SENSOR:
 DC SCALE FACTOR - 4.360 (VOLTS/PSI)
 DC PHASE (DEGREES) - 180.0
 POLE FREQ (HZ) - 2880.

PREAMPLIFIER:
 DC GAIN (DB) - -63.14 DC PHASE (DEG) - 0.0000
 ZERO FREQ (HZ) - 0.1000E-04
 POLE FREQ (HZ) - 0.2830E-01
 POLE FREQ (HZ) - 100.0 DAMP COEFF - 0.7070

FILTER:
 STAGE 1
 DC GAIN (DB) - 7.087 DC PHASE (DEG) - 0.0000
 POLE FREQ (HZ) - 670.0
 STAGE 2
 DC GAIN (DB) - 0.1116E-02 DC PHASE (DEG) - 180.0
 POLE FREQ (HZ) - 34.30 DAMP COEFF - 1.000
 STAGE 3
 DC GAIN (DB) - 0.9406E-02 DC PHASE (DEG) - 0.0000
 POLE FREQ (HZ) - 34.40 DAMP COEFF - 0.7322
 STAGE 4
 DC GAIN (DB) - 0.0662E-02 DC PHASE (DEG) - 180.0
 POLE FREQ (HZ) - 1590.
 STAGE 5
 DC GAIN (DB) - -0.2719E-01 DC PHASE (DEG) - 180.0
 POLE FREQ (HZ) - 34.37 DAMP COEFF - 0.2670



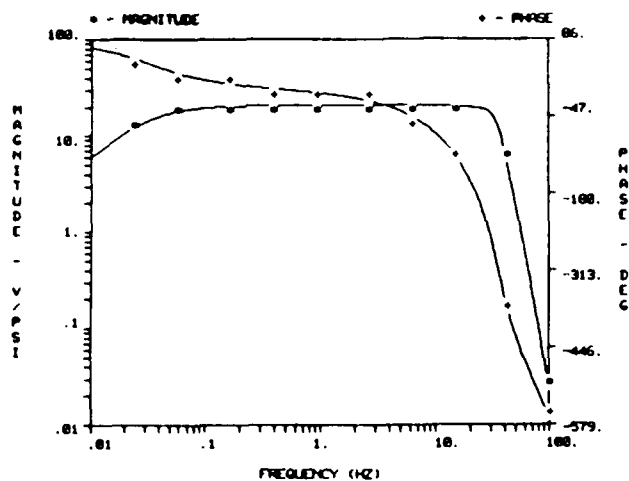
CHANNEL RESPONSES

CHANNEL 13

SENSOR:
 DC SCALE FACTOR = 4.660 (VOLTS/PSI)
 DC PHASE (DEGREES) = 100.0
 POLE FREQ (HZ) = 2000.

PREAMPLIFIER:
 DC GAIN (DB) = -64.56 DC PHASE (DEG) = 0.0000
 ZERO FREQ (HZ) = 0.1000E-04 DAMP COEFF = 0.7070
 POLE FREQ (HZ) = 0.3330E-01
 POLE FREQ (HZ) = 100.0

FILTER:
 STAGE 1
 DC GAIN (DB) = 7.092 DC PHASE (DEG) = 0.0000
 POLE FREQ (HZ) = 670.0
 STAGE 2
 DC GAIN (DB) = 0.0000 DC PHASE (DEG) = 100.0
 POLE FREQ (HZ) = 34.30 DAMP COEFF = 1.000
 STAGE 3
 DC GAIN (DB) = 0.0000 DC PHASE (DEG) = 0.0000
 POLE FREQ (HZ) = 34.30 DAMP COEFF = 0.7342
 STAGE 4
 DC GAIN (DB) = 0.0000 DC PHASE (DEG) = 100.0
 POLE FREQ (HZ) = 1592.
 STAGE 5
 DC GAIN (DB) = 0.0000 DC PHASE (DEG) = 100.0
 POLE FREQ (HZ) = 34.30 DAMP COEFF = 0.2579

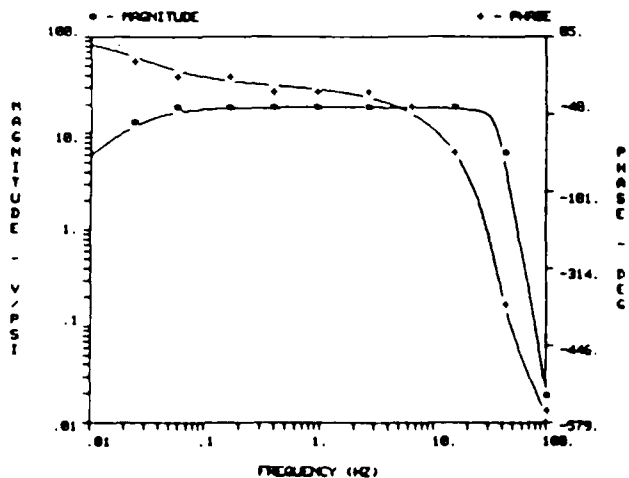


CHANNEL 14

SENSOR:
 DC SCALE FACTOR = 4.710 (VOLTS/PSI)
 DC PHASE (DEGREES) = 100.0
 POLE FREQ (HZ) = 2000.

PREAMPLIFIER:
 DC GAIN (DB) = -63.90 DC PHASE (DEG) = 0.0000
 ZERO FREQ (HZ) = 0.1000E-04 DAMP COEFF = 0.7070
 POLE FREQ (HZ) = 0.2970E-01
 POLE FREQ (HZ) = 100.0

FILTER:
 STAGE 1
 DC GAIN (DB) = 6.030 DC PHASE (DEG) = 0.0000
 POLE FREQ (HZ) = 670.0
 STAGE 2
 DC GAIN (DB) = 0.0000 DC PHASE (DEG) = 100.0
 POLE FREQ (HZ) = 34.30 DAMP COEFF = 1.000
 STAGE 3
 DC GAIN (DB) = 0.0000 DC PHASE (DEG) = 0.0000
 POLE FREQ (HZ) = 34.30 DAMP COEFF = 0.7342
 STAGE 4
 DC GAIN (DB) = 0.0000 DC PHASE (DEG) = 100.0
 POLE FREQ (HZ) = 1592.
 STAGE 5
 DC GAIN (DB) = 0.0000 DC PHASE (DEG) = 100.0
 POLE FREQ (HZ) = 34.30 DAMP COEFF = 0.2579



CHANNEL RESPONSES

CHANNEL 15

SENSOR:
 DC SCALE FACTOR - 4.220 (VOLTS/PSI)
 DC PHASE (DEGREES) - 180.0
 POLE FREQ (HZ) - 2000.

PREAMPLIFIER:
 DC GAIN (DB) - -64.11 DC PHASE (DEG) - 0.0000
 ZERO FREQ (HZ) - 0.1000E-04
 POLE FREQ (HZ) - 0.3160E-01 DAMP COEFF - 0.7070
 POLE FREQ (HZ) - 100.0

FILTER:

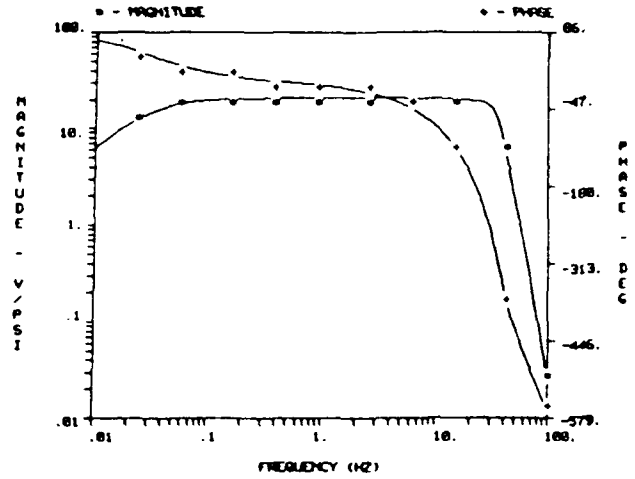
STAGE 1
 DC GAIN (DB) - 7.915 DC PHASE (DEG) - 0.0000
 POLE FREQ (HZ) - 670.0

STAGE 2
 DC GAIN (DB) - 0.0000 DC PHASE (DEG) - 180.0
 POLE FREQ (HZ) - 34.30 DAMP COEFF - 1.000

STAGE 3
 DC GAIN (DB) - 0.0000 DC PHASE (DEG) - 0.0000
 POLE FREQ (HZ) - 34.30 DAMP COEFF - 0.7342

STAGE 4
 DC GAIN (DB) - 0.0000 DC PHASE (DEG) - 180.0
 POLE FREQ (HZ) - 1592.

STAGE 5
 DC GAIN (DB) - 0.0000 DC PHASE (DEG) - 180.0
 POLE FREQ (HZ) - 34.30 DAMP COEFF - 0.2679



CHANNEL 16

SENSOR:
 DC SCALE FACTOR - 4.750 (VOLTS/PSI)
 DC PHASE (DEGREES) - 180.0
 POLE FREQ (HZ) - 2000.

PREAMPLIFIER:
 DC GAIN (DB) - -63.15 DC PHASE (DEG) - 0.0000
 ZERO FREQ (HZ) - 0.1000E-04
 POLE FREQ (HZ) - 0.2830E-01 DAMP COEFF - 0.7070
 POLE FREQ (HZ) - 100.0

FILTER:

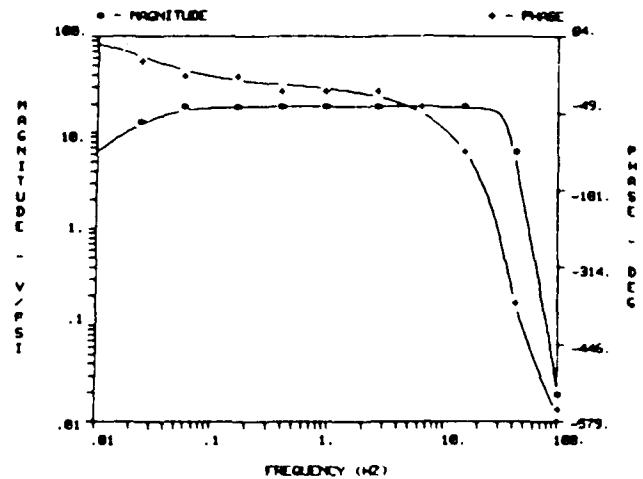
STAGE 1
 DC GAIN (DB) - 6.830 DC PHASE (DEG) - 0.0000
 POLE FREQ (HZ) - 670.0

STAGE 2
 DC GAIN (DB) - 0.0000 DC PHASE (DEG) - 180.0
 POLE FREQ (HZ) - 34.30 DAMP COEFF - 1.000

STAGE 3
 DC GAIN (DB) - 0.0000 DC PHASE (DEG) - 0.0000
 POLE FREQ (HZ) - 34.30 DAMP COEFF - 0.7342

STAGE 4
 DC GAIN (DB) - 0.0000 DC PHASE (DEG) - 180.0
 POLE FREQ (HZ) - 1592.

STAGE 5
 DC GAIN (DB) - 0.0000 DC PHASE (DEG) - 180.0
 POLE FREQ (HZ) - 34.30 DAMP COEFF - 0.2679

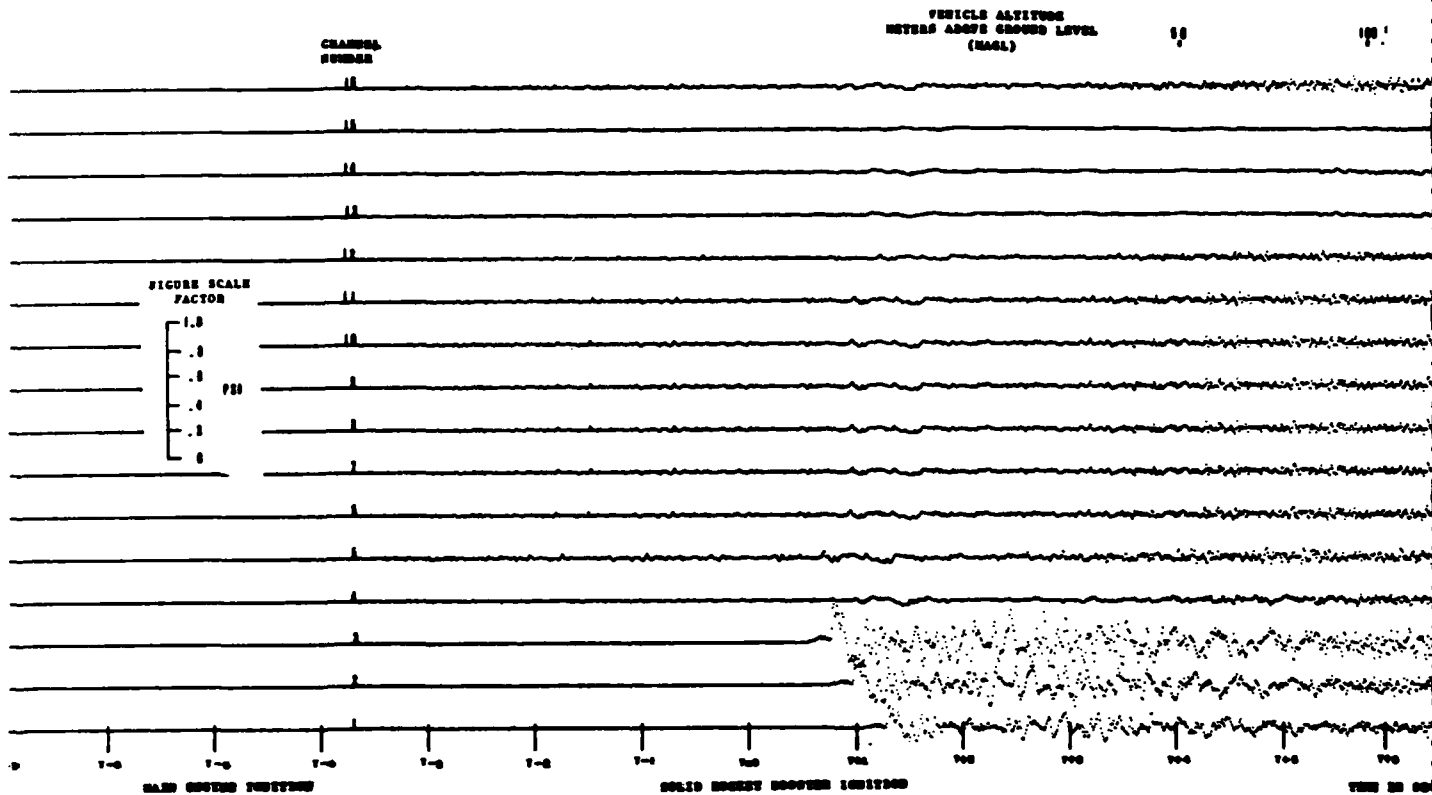


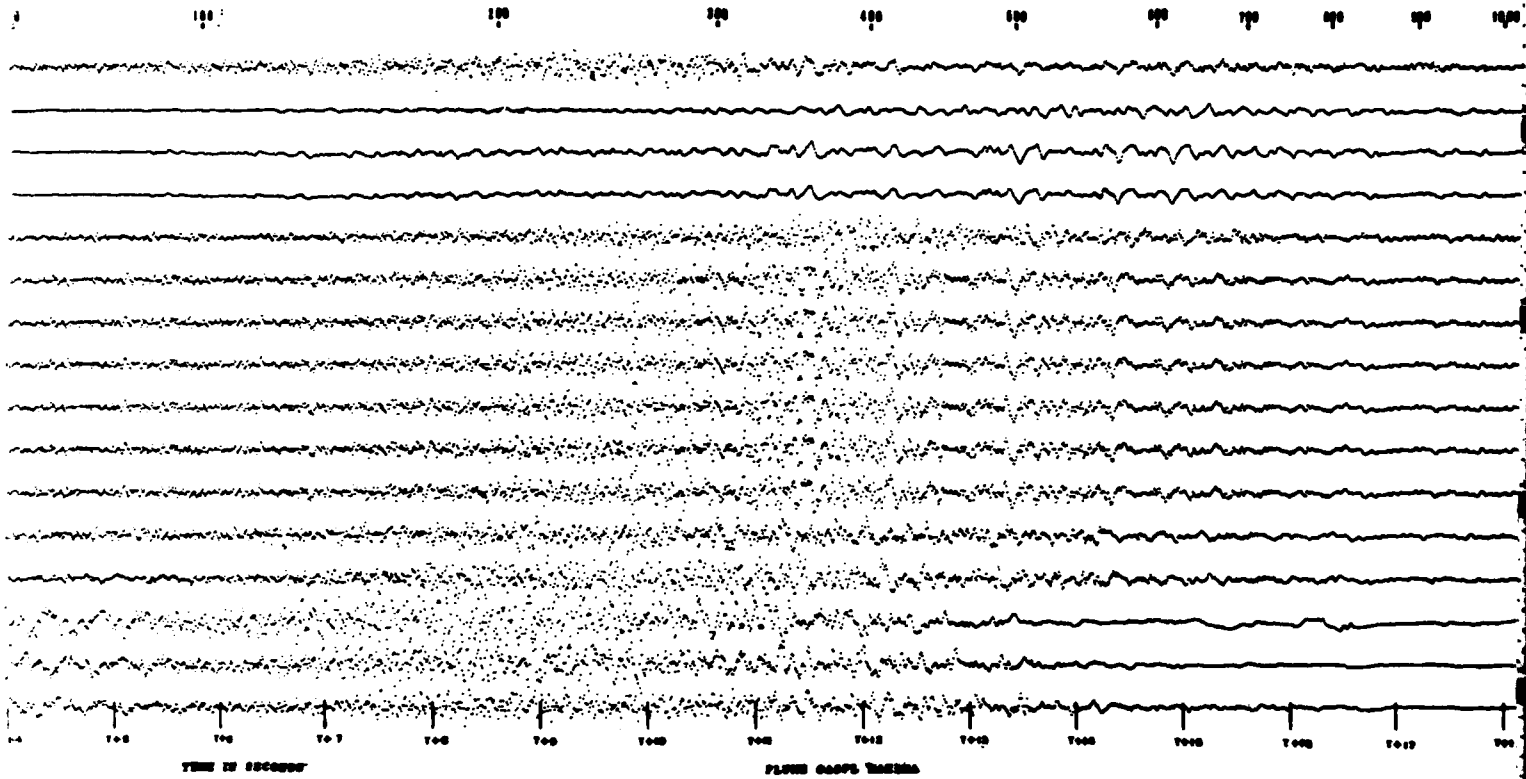
CHANNEL RESPONSES

9.2 APPENDIX B, GLOSSARY

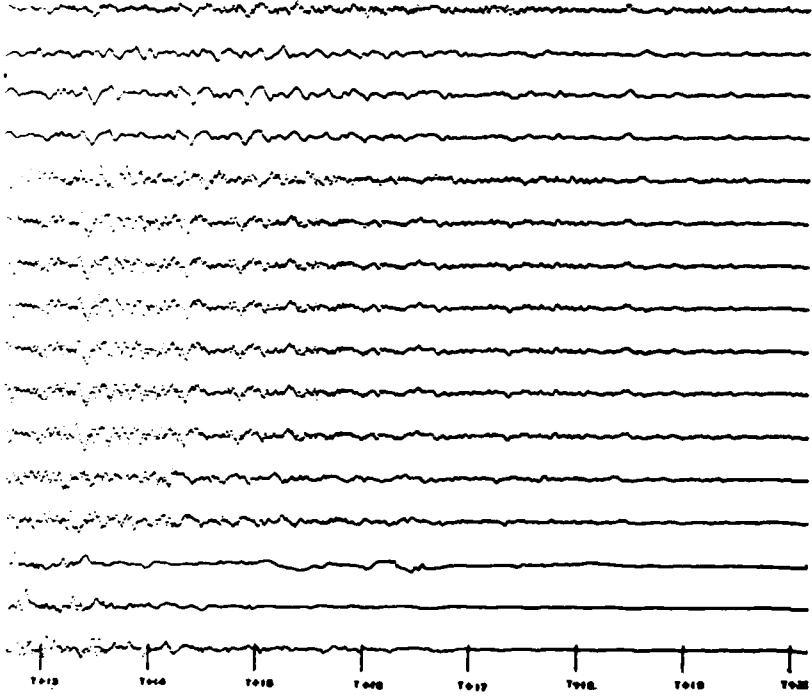
AFGL	Air Force Geophysics Laboratory
Az	Azimuth
C	Phase velocity
C_0	Speed of sound in air
Ch	Channel
db	Decibel
DOF	Degrees of freedom
f	Frequency
f_m	Frequency of $G_{pp}(f)$ maximum
f_N	Nyquist frequency
f_l	GDAS low frequency cutoff
f_h	GDAS high frequency
G	Midband Gain
GDAS	Geokinetic Data Acquisition System
Gmax	Spectral maximum
$G_{pp}(f)$	Theoretical undeflected plume spectrum
GSS	Ground Support System
i	$\sqrt{-1}$
k	Wave number
λ	Integer
KSC	Kennedy Space Center
LCC	Launch Control Center
NASA	National Aeronautics & Space Administration
θ_s	Source phase
OASPL	Overall sound power level
p	Pressure

$p(p-p)$	Peak to peak pressure
$p(R,t)$	Pressure at distance R, at time t, from acoustic source
$p(r,t)$	Pressure at distance r, at time t, from launch pad
$p(r,\omega)$	Fourier transform of $p(r,t)$
PSI	Pounds per sq. in.
R	Range
SD	Space Division
S/N	Signal to noise ratio
SPL	Sound power level
SPL (25)	Sound power level, frequencies less than 25 Hz
SRB	Solid Rocket Booster
STS	Space Transportation System
T	Time after lift-off, seconds
T_o	Lift-off time
t	Time
VAFB	Vandenberg Air Force Base
$V_o(p-p)$	Peak to peak volts
$\gamma(k,\omega)$	Ratio of magnitude of k weighted sum and scalar sum for $p(r_l, \omega)$
$\hat{\gamma}(k,\omega)$	Absolute maximum of $\gamma(k,\omega)$
τ_p	Phase delay
ω	Angular frequency $\omega=2\pi f$





100 200 300 400 500 600



3

END

FILMED

4-85

DTIC